Received: 17 May 2021 | Revised: 17 June 2021 | Accepted: 23 June 2021

DOI: 10.1002/ar.24731

FULL LENGTH ARTICLE

The Anatomical Record | WILEY

New specimens provide insights into the anatomy of the dinosauriform *Lewisuchus admixtus* Romer, 1972 from the upper Triassic levels of the Chañares Formation, NW Argentina

Federico Agnolín[1,2] | **Federico Brissón Egli**[1] | **Martín D. Ezcurra**[3] | **Max C. Langer**[4] | **Fernando Novas**[1]

[1]Laboratorio de Anatomía Comparada y Evolución de los Vertebrados, CONICET–Museo Argentino de Ciencias Naturales "Bernardino Rivadavia,", Buenos Aires, Argentina

[2]Fundación de Historia Natural "Félix de Azara," Departamento de Ciencias Naturales y Antropología, Universidad Maimónides, Buenos Aires, Argentina

[3]Sección Paleontología de Vertebrados, CONICET–Museo Argentino de Ciencias Naturales "Bernardino Rivadavia", Buenos Aires, Argentina

[4]Departamento de Biologia-FFCLRP, Universidade de São Paulo, Ribeirão Preto, São Paulo, Brazil

Correspondence
Federico Agnolín, Laboratorio de Anatomía Comparada y Evolución de los Vertebrados, CONICET–Museo Argentino de Ciencias Naturales "Bernardino Rivadavia" Av. Ángel Gallardo 470 (C1405DJR), Buenos Aires, Argentina.
Email: fedeagnolin@yahoo.com.ar

Funding information
Mr. Coleman Burke (New York); Agencia Nacional de Investigaciones Científicas y Técnicas, Grant/Award Numbers: PICT 2018-1390, PICT 2018-1186

Abstract

Lewisuchus admixtus is an early dinosauriform described by Alfred Romer in 1972 on the basis of a single, incomplete skeleton, collected in lower Upper Triassic rocks of the renowned Chañares Formation, at the Los Chañares type-locality, La Rioja Province, north-western Argentina. Recent field explorations to the type-locality resulted in the discovery of two partial articulated skeletons, which provide significant novel information. The cranial bones, presacral series, femur, tibia, and proximal tarsals of the new specimens match the preserved overlapping anatomy of the holotype and previously referred specimens of *L. admixtus*, including the presence of unique combination of character states among dinosauriforms (anterior presacral column with additional ossification on the top of neural spines, dorsal neural spines fan-shaped, anterior surface of the astragalus with a dorsally curved groove, and an inflated area on the anterior portion of the medial surface of this bone). This new information improves our understanding of the anatomy and taxonomy of early dinosauriforms and reinforces the role of Argentinean beds on the study of the origin of dinosaurs.

KEYWORDS

Archosauria, Dinosauriformes, Late Triassic, *Lewisuchus admixtus*, South America

Institutional Abbreviations: CRILAR-Pv, Centro Regional de Investigaciones y Transferencia Tecnológica de La Rioja, Paleontología de Vertebrados, Anillaco, La Rioja, Argentina; MACN-Pv, Museo Argentino de Ciencias Naturales "Bernardino Rivadavia," Paleontología de Vertebrados, Buenos Aires, Argentina; MB, Museum für Naturkunde—Leibniz-Institut für Evolutions—und Biodiversitätsforschung, Berlin, Germany; MCP, Museu de Ciências e Tecnologia da Pontifícia Universidade Católica do Rio Grande do Sul, Porto Alegre, Brazil; MCZ, Museum of Comparative Zoology, Cambridge, USA; PULR, Paleontología, Universidad Nacional de La Rioja, La Rioja, Argentina; PVL, Paleontología de Vertebrados, Instituto "Miguel Lillo," San Miguel de Tucumán, Argentina; ULBRA, Museu de Ciências Naturais, Universidade Luterana do Brasil, Canoas, Brazil; ZPAL, Institute of Paleobiology of the Polish Academy of Sciences, Warsaw, Poland.

1 | INTRODUCTION

Lewisuchus admixtus was described by Romer (1972) on the basis of a single skeleton represented by a partial skull and postcranium, lacking the pelvic girdle and most of the hindlimb. This holotypic specimen comes from the lower Carnian rocks of the type-locality of the renowned Chañares Formation, Talampaya National Park, La Rioja Province, north-western Argentina (Bittencourt, Arcucci, Marsicano, & Langer, 2014; Romer, 1972). These beds yielded several avian-line archosaurs (e.g., *Lagerpeton chanarensis*, *Lagosuchus talampayensis*) that are, together with silesaurids (Dzik, 2003; Ferigolo & Langer, 2007; Nesbitt et al., 2010), the best-known ornithodirans predating the Late Triassic radiation of dinosaurs (Bonaparte, 1975; Sereno & Arcucci, 1993, 1994). These taxa allowed the recognition of two main ornithodiran clades, Dinosauromorpha (Benton, 1985) and Dinosauriformes (Novas, 1992), and continue to clarify the acquisition sequence of dinosaurian synapomorphies (e.g., Ezcurra, Nesbitt, Fiorelli, 2020; Ezcurra, Fiorelli, Bronzati, 2020; Langer, Ezcurra, Bittencourt, & Novas, 2010; Novas et al., 2021; Sereno & Arcucci, 1993, 1994).

In its original description, Romer (1972) proposed that *L. admixtus* was probably related to the ancestry of Coelurosauria (i.e., lightly built theropods; Gauthier, 1986), whereas later authors considered it as a sphenosuchian crocodylomorph of uncertain affinities (Bonaparte, 1982, 1997; Mattar, 1987). More recently, Arcucci (1997, 1998, 2005) proposed that *L. admixtus* could be a nondinosaurian dinosauriform, and suggested its potential synonym with "*Pseudolagosuchus major*" (Arcucci, 1987). This hypothesis of synonym was also discussed by subsequent authors (e.g., Ezcurra & Martínez, 2016; Hutchinson, 2001; Langer & Benton, 2006; Nesbitt, 2011; Nesbitt et al., 2010), but it could not be objectively tested because the hypodigms of both taxa lack informative overlapping skeletal parts. Bittencourt et al. (2014) redescribed in detail the holotype of *L. admixtus*, argued in favor of its position among nondinosaurian dinosauriforms, but did not endorse its synonymy with "*Pseudolagosuchus major*." More recently, Ezcurra, Nesbitt, Fiorelli et al. (2020) described a new *L. admixtus* specimen from the Chañares Formation that preserves overlapping bones with the holotypes of both *L. admixtus* and "*Pseudolagosuchus major*." This specimen added novel anatomical information of several portions of the skeleton (e.g., skull and forelimb) and allowed Ezcurra, Nesbitt, Fiorelli et al. (2020) to formally propose that "*Pseudolagosuchus*" and "*Pseudolagosuchus major*" are junior subjective synonyms of *Lewisuchus* and *L. admixtus*, respectively. Despite some phylogenetic studies concluding that *L. admixtus* is a member of Silesauridae (Ezcurra, Nesbitt, Fiorelli et al., 2020; Nesbitt et al., 2010), more recent authors raised doubts about this proposal (Novas et al., 2021), and, thus, the phylogenetic position of *L. admixtus* among dinosauriforms is still on debate.

Novas, Agnolín, and Ezcurra (2015) preliminary reported the discovery of a new partial dinosauriform skeleton (PULR V-111) from the same levels as the holotype of *L. admixtus* and referred it to this species. García-Marsà, Agnolín, and Novas (2019) described the osteohistology of this specimen and that of an additional one (PULR V-113) that was also referred to *L. admixtus*. Here, we describe and compare in detail these two specimens and discuss their taxonomy.

2 | GEOLOGICAL AND PALAEONTOLOGICAL BACKGROUND

The Chañares Formation represents the lowermost unit of the Agua de la Peña Group (Kokogian et al., 2001; Milana & Alcober, 1995) and rests on an unconformity with the Tarjados Formation (Ezcurra et al., 2017; Fiorelli et al., 2013; Rogers et al., 2001), within the Ischigualasto-Villa Unión Basin (Kokogian et al., 2001; Stipanicic & Bonaparte, 1972). In the area of the Talampaya National Park, the outcrops of the Chañares Formation are relatively small and separated from one another, being controlled by small north-south oriented faults (Romer & Jensen, 1966). In the "Romer site" (29°49′8.9″S, 67°48′47.9″W; Figure 1), most fossil vertebrates come from the lower 6–30 m of exposed outcrop (Ezcurra et al., 2017; Fiorelli et al., 2013), which is rich in medium-sized to large (diameter between 30 cm and 2.5 m) subspherical concretions (Mancuso, Gaetano, Leardi, Abdala, & Arcucci, 2014). These concretions preserve abundant vertebrate fossils, including nearly complete skeletons of pseudosuchians, cynodonts, dicynodonts, proterochampsids, and dinosauriforms (Bonaparte, 1997; Mancuso et al., 2014; Rogers et al., 2001; Romer & Jensen, 1966). The depositional environment of the Chañares Formation was interpreted as a flood plain (Mancuso & Caselli, 2012; Milana & Alcober, 1995; Rogers et al., 2001).

Based on long-range vertebrate biostratigraphy, most authors considered the Chañares Formation as late Middle Triassic in age, probably equivalent to the Ladinian stage of the European chronostratigraphy (see Bonaparte, 1997; Langer et al., 2010). More recently, a younger Ladinian–early Carnian age has been proposed

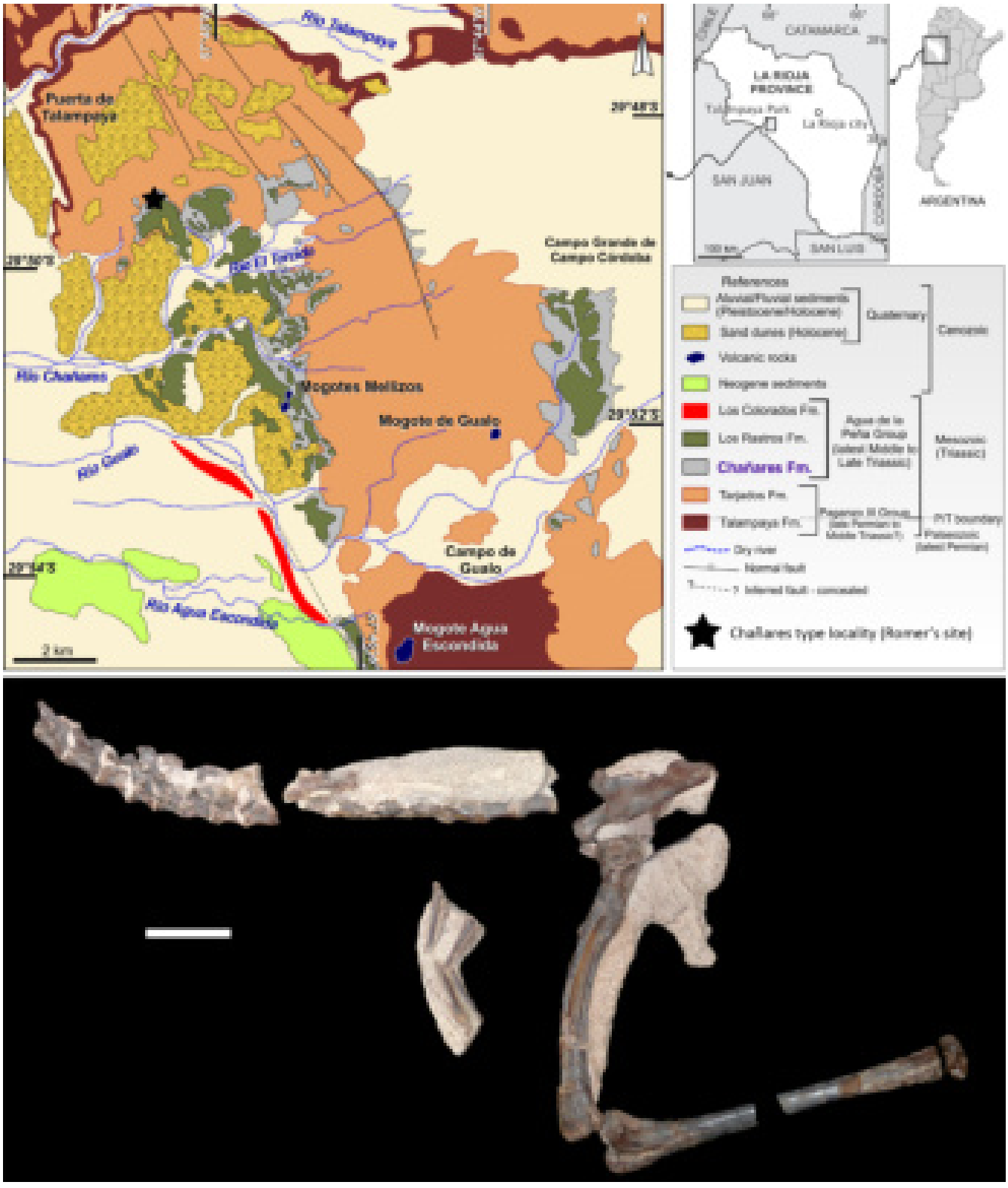

FIGURE 1 Top, geographic position of the Chañares type locality (Romer's site) in a geological map of the Chañares Formation in the area of the Talampaya National Park that yielded the specimens of *Lewisuchus admixtus* (PULR V-111 and PULR V-113) here described. Bottom, preserved bones of PULR V-111. Scale bar: 2 cm. Map modified from Ezcurra, Fiorelli, Trotteyn, et al. (2020)

by Desojo, Ezcurra, and Schultz (2011). The first absolute dates of the Chañares Formation show that it is mostly Carnian in age (Marsicano, Irmis, Mancuso, Mundil, & Chemale, 2016), but the Ladinian-Carnian boundary probably occurs within the first meters of the unit (Ezcurra et al., 2017).

3 | MATERIALS AND METHODS

We follow the phylogenetic nomenclature and topology of early pan-avians proposed by Ezcurra, Nesbitt, Bronzati, et al. (2020), for example, lagerpetids are included within Pterosauromorpha instead of Dinosauromorpha. We also follow Agnolín and Ezcurra (2019), who considered "*Marasuchus lilloensis*" (Romer, 1972) as a junior synonym of *L. talampayensis* (Romer, 1971), in agreement with Bonaparte (1975). Finally, we follow the formal proposal of synonym between "*Pseudolagosuchus*" and "*Pseudolagosuchus major*" Arcucci, 1987 and *Lewisuchus* and *L. admixtus* Romer, 1972, respectively (Ezcurra, Nesbitt, Fiorelli, et al., 2020).

Vertebral laminae and fossae nomenclature follows Wilson (1999) and Wilson, Michael, Ikejiri, Moacdieh, and Whitlock (2011), respectively.

4 | SYSTEMATIC PALAEONTOLOGY

Archosauria Cope, 1869 (Gauthier & Padian, 2020).

Pan-Aves Gauthier & de Queiroz, 2001 (Ezcurra, Nesbitt, Bronzati, et al., 2020).

Dinosauriformes Novas, 1992 (Ezcurra, Nesbitt, Bronzati, et al., 2020).

L. admixtus Romer, 1972.

4.1 | Holotype

PULR 01, partial skeleton, including both cranial and postcranial bones. See Bittencourt et al. (2014) and Ezcurra, Nesbitt, Fiorelli, et al. (2020) for a complete list of elements.

4.2 | Newly referred specimens

PULR-V 111, partially articulated skeleton composed of complete left postorbital, incomplete left squamosal and quadrate, several presacral vertebrae (Cv5–D3 and D4–D10), dorsal ribs, left ilium, pubis, ischium, femur, tibia, astragalus, and calcaneum (Figure 1). This specimen was preliminary reported by Novas et al. (2015). PULR-V 113, a sacrum articulated to left ilium and proximal region of both pubes, both ischia, and incomplete left femur and tibia. The palaeohistology of both specimens was described by García Marsá et al. 2019). See Ezcurra, Nesbitt, Fiorelli, et al. (2020) for an expanded list of specimens.

4.3 | Locality and horizon

PULR-V 111 and PULR-V 113 were collected in 2013 from the "type locality" of the Chañares Formation (see Romer & Jensen, 1966), in an area delimited by the Chañares and Gualo rivers, which is currently known as "Romer's site" (Figure 1). This fossiliferous site is located 3 km to the north of the north branch of the Chañares river and 5 km to the southwest of the Puerta de Talampaya (Romer, 1972; Sereno & Arcucci, 1994), La Rioja Province, north-western Argentina. See Ezcurra, Nesbitt, Fiorelli, et al. (2020) for a comprehensive description of the geographic and geological occurrences of the hypodigm of *L. admixtus*.

4.4 | Diagnosis

Modified from Ezcurra, Nesbitt, Fiorelli, et al. (2020): proportionally large skull, in which the length of the maxilla equals 0.71 the length of the scapula and 0.61 the length of the tibia; premaxillary tooth crowns conical and without serrations; first seven maxillary tooth crowns without mesiodistally expanded bases and mesial serrations, with distal serrations orthogonal to the margin of the crown, and four faint and nearly longitudinal ridges at the base of the crown that converge toward the apex on both lingual and labial surfaces; three foramina posterior to the metotic strut; anteroposteriorly extending rugose ridge on the middle height of the lateral surface of the axial neural spine; coracoid portion of the glenoid fossa slanting mainly laterally; absence of coracoid foramen, at least in the posterior two-thirds of the bone; pubes with a rodlike shaft and a median notch between their distal ends, so that the distalmost ends of the pubes do not meet on the midline; femoral head without a longitudinal groove on its proximal surface, has a well-developed trochanteric fossa and anteromedial tuber, and is moderately medially offset, with a square profile, and a notch separating it from the shaft in anterior or posterior view; femur with a popliteal fossa that extends proximally less than 1/4 the length of the bone; fibula with a tab-like, medially projected process at the level of the iliofibularis tubercle; astragalus with subequally projected anterolateral and posterolateral processes, and without a well-rimmed fossa posterior to the ascending process; calcaneum with a calcaneal tuber poorly posteriorly projected from the fibular facet; presence of a single row of elongated osteoderms on the distal surface of the postaxial cervical and, at least, first nine dorsal neural spines.

Here, we add the following autapomorphy for the species: postorbital with a low and broad ridge on the

lateral surface of its main body, extending posterodorsally from the orbital margin onto the posterior process and being dorsally and ventrally delimited by depressions that extend onto the surfaces of the dorsal and ventral processes, respectively.

4.5 | Comments

PULR V-111 and V-113 are referred to *L. admixtus* on the basis of the following unique combination of character states shared with the holotype and previously referred specimens, but absent in other Triassic archosaurs: ilium with a shallow and ventrally facing brevis fossa; femoral head without a longitudinal groove on its proximal surface, with a well-developed trochanteric fossa and anteromedial tuber, moderately medially offset, with a square profile, and a notch separating it from the shaft in anterior or posterior views; and femur with a popliteal fossa that extends proximally less than 1/4 the length of the bone. In addition, PULR V-111 has a postorbital with a low and broad ridge on the lateral surface of its main body that is dorsally and ventrally delimited by depressions (also present in the holotype of the species) and a single row of elongated osteoderms on the dorsal surface of neural spines of postaxial cervical and anterior-middle dorsal vertebrae. The former character state is proposed here as an autapomorphy of *L. admixtus* and the latter has been considered an autapomorphy of the species by previous authors (Bittencourt et al., 2014; Ezcurra, Nesbitt, Fiorelli, et al., 2020).

5 | DESCRIPTION

The following description is mainly based on PULR V-111, which is the most complete and well-preserved of the new specimens. The description of the sacrum is based on PULR V-113 and this specimen also complements the iliac morphology.

5.1 | Postorbital

The left postorbital is fairly complete, lacking the tips of the anterior, posterior, and ventral processes (Figure 2; Table 1). It is a triradiate bone, that delimits a broadly concave posterodorsal border of the orbit, a squared anterodorsal corner of the infratemporal fenestra, and an obtuse-angled anterolateral border of the supratemporal fenestra. The orbital margin bears an anterolaterally oriented flange forming a low, tab-like spur that projects into de orbit in lateral view. The lateral surface of this flange has a rugose ornamentation sub-perpendicular to the orbital margin. The orbit excavates the anterior surface of the postorbital and, as a result, the orbital cavity is partially obscured in lateral view.

FIGURE 2 Fairly complete left postorbital of *Lewisuchus admixtus* (PULR V-111) in: (a), lateral; (b), anterior; (c), medial; (d), posterior and E, dorsal views. References: ad, anterior depression; amc, anteromedial crest; ap, anterior process; ff, frontal or postfrontal facet; jf, jugal facet; lc, lateral crest; o, orbital wall; of, orbital flange; pmc, posteromedial crest; pp, posterior process; vp, ventral process. Scale bar: 1 cm

TABLE 1 Measurements (in mm) of the cranial bones of *Lewisuchus admixtus* (PULR V-111)

Left postorbital	
Anteroposterior length	(14.9)
Dorsoventral height	(24.6)
Left squamosal	
Dorsoventral height	(11.6)
Anteroposterior width of ventral process	3.3
Length of ventral process	(4.7)
Left quadrate	
Dorsoventral height	23.6
Left pterygoid	
Anteroposterior length	(15.5)
Dorsoventral height	(10.2)
Minimum width at base of quadrate ramus	5.0

Note: Values between brackets indicate incomplete measurements (due to postmortem damage) and the value given is the maximum measurable. Maximum deviation of the calliper is 0.02 mm but measurements were rounded to the nearest 0.1 mm.

The anterior process of the postorbital is almost completely lost in the holotype of *L. admixtus* (PULR 01). In PULR V-111, it is notably elongated, representing more than 50% of the length of the ventral process (but its tip is also missing). The anterior process is anterodorsally oriented and gently dorsally arched in lateral view. Its dorsal surface has a thick, transversely convex longitudinal ridge that delimits the articulation facet for the frontal and extends posteriorly along the entire dorsal margin of the bone. The lateral surface of the anterior process possesses a shallow depression extending along its posterior two-thirds and disappears at the

distalmost preserved portion. This depression is ventrally delimited by the orbital flange. The medial surface of the process is mostly occupied by a well-defined concavity that received the posterolateral corner of the frontal. The anterior process is sub-triangular in cross-section, with straight lateral and medial margins and weakly convex ventral margin.

At least the posterior half of the posterior process of the postorbital is missing in the holotype of *L. admixtus* (PULR 01). That process in PULR V-111 is subtriangular in lateral view, tapering posteriorly, and (if the ventral process is vertically aligned) positioned distinctly below the level of the anterior process of the bone. The lateral and medial surfaces of the posterior process are smooth and mostly flat. Its ventral surface is transversely concave and delimited laterally and medially by sharp edges. The dorsal surface is damaged, but strongly transversely convex as preserved. The posterior process is sub-triangular in cross-section with flat lateral and medial surfaces and a concave ventral one.

The ventral process is the longest of the postorbital. It is posteriorly convex when viewed from the sides; the orbital margin is mostly concave, except for the tab-like flange, which is anteriorly convex. The lateral surface of the ventral process is smooth, slightly transversely concave along most of its preserved length, and becomes transversely convex at its distalmost preserved portion. The jugal articulation is incompletely preserved, being represented by a groove on its posterior surface, indicating a diagonal, anteroventrally-to-posterodorsally oriented suture, as occurs in the holotype of *L. admixtus* (Romer, 1972). The ventral process is sub-triangular in cross-section, with straight margins and a posteriorly oriented apex.

The lateral surface of the main body of the postorbital possesses a low and broad ridge that extends posterodorsally from the orbital margin onto the posterior process. This crest is dorsally and ventrally delimited by depressions that extend onto the surfaces of the dorsal and ventral processes, respectively. The same ridge and depressions are present in the holotype of *L. admixtus* (PULR 01) and seems to represent an autapomorphy of the species. In medial view, the postorbital has a well-developed and sharp semilunate crest that separates the temporal from the orbital region (Sampson & Witmer, 2007). The facet for articulation with the laterosphenoid is not preserved, but it was likely present immediately posteroventral to the facet for the frontal on the semilunate ridge, at the base of the anterior process. Indeed, in this area, the semilunate ridge is broken and may have housed a medial projection for contact with the capitate process of the laterosphenoid.

5.2 | Squamosal

A partial left squamosal is preserved in articulation with the quadrate, missing the posterior process, and the distal ends of the anterior, medial, and ventral processes (Figure 3; Table 1). Thus, the bone is more completely preserved than that of the holotype of *L. admixtus*, with the exception of the posterior process, which preserves its proximal half in the holotype (Romer, 1972). The squamosal of PULR V-111 forms a strongly concave posterodorsal corner of the infratemporal fenestra in lateral view. As preserved, the anterior and ventral processes form an approximately right angle to one another. However, when the quadrate is oriented close to the vertical (as in PULR 01), the preserved base of the anterior process of the squamosal becomes anterodorsally oriented. As a result, the unpreserved part of that process in PULR V-111 would have been ventrally curved in order to articulate with the posterior process of the postorbital, resulting in an acute angle between the main bodies of the anterior and ventral processes. This inferred condition resembles that seen in some early dinosaurs (e.g., *Pampadromaeus barberenai*: ULBRA-PVT016; *Saturnalia tupiniquim*: MCP 3845-PV). The posteriormost preserved region of the squamosal is transversely narrow and possesses a deep socket for articulation with the quadrate head, which is laterally exposed. This socket is medially delimited by the preserved portion of the base of the posterior process, which is only represented by a small and sub-triangular portion of bone. The dorsal and dorsolateral surfaces of the squamosal are convex and separated from the lateral surface by a low, thick, and anterodorsally-to-posteroventrally oriented ridge. Below this ridge, the lateral surface of the squamosal is slightly excavated along the ventral process and becomes anteroposteriorly convex at the distalmost preserved

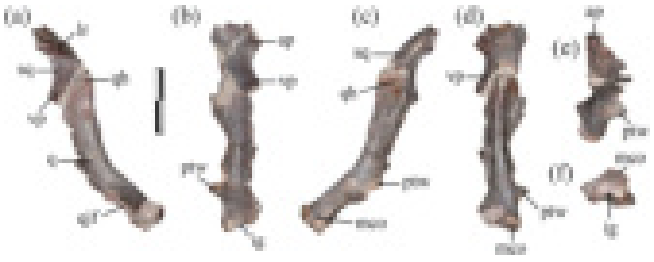

FIGURE 3 Partial left quadrate and squamosal of *Lewisuchus admixtus* (PULR V-111) in: (a), lateral; (b), anterior; (c), medial; (d), posterior; (e), dorsal and F, ventral views. References: ap, anterior process; ig, intercondylar groove; lr, lateral ridge; mdc, mediodistal condyle; lr, lateral ridge; mco, medial condyle; ptw, pterygoid wing; q, quadrate; qh, quadrate head; qjf, quadratojugal facet; sq, squamosal; vp, ventral process. Scale bar: 1 cm

region of the process. The ventral process was probably anteroventrally oriented (see above). The preserved portion of the medial process is dorsoventrally low and anteromedially oriented, with a transversely convex dorsal surface and a concave ventral one. Thus, the squamosal lacks a supratemporal fossa. The inner surface of the squamosal is deeply concave, especially at its main body.

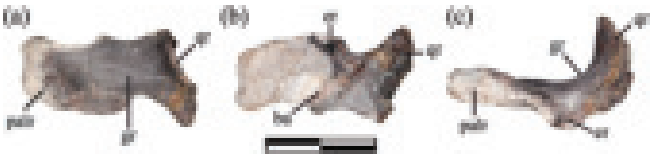

FIGURE 4 Partial left pterygoid of *Lewisuchus admixtus* (PULR V-111) in: (a), dorsal; (b), ventral; and (c), medial views. References: ba, basal articulation; er, ectopterygoid ramus; gr, groove; palr, palatine ramus; qr, quadrate ramus. Scale bar: 1 cm

5.3 | Quadrate

The left quadrate lacks most of the pterygoid wing and part of the lateral condyle, and the dorsal two-thirds of the lateral margin of the bone are damaged (Figure 3; Table 1). The quadrate is anteriorly arched in lateral view and the quadrate shaft is crescent-shaped in cross-section, with an anteriorly facing concave margin. There are two laminae that arise from the quadrate shaft. One of them is anteriorly and slightly laterally projected, nearly straight in cross-section, and should have received the distal half of the ventral process of the squamosal and the dorsal process of the quadratojugal. The other lamina is anteromedially oriented, anterolaterally arched in cross-section, and represents the base of the pterygoid wing. The preserved region of the squamosal articulation is anteroventrally-to-posterodorsally oriented and straight. The quadrate shaft is weakly sigmoid in posterior view, with a medially concave dorsal half and a weakly laterally concave ventral half. The anterior surface of the quadrate possesses a distinct posterior inflection proximal to the ventral condyles. At level of this inflection, the posterior surface of the bone has a low, mound-like prominence.

The ventral end of the bone differs from its shaft in being strongly anteriorly concave. The articulation surface for the quadratojugal is subrectangular, gently concave, and medially placed with respect to the anterolateral flange. In medial view, the pterygoid wing reaches the ventral end of the bone, but it does not contact the ventral condyles. The ventral surface is composed of two articular condyles. The medial one is kidney-shaped, with an anteroposterior main axis, and projects anteriorly beyond the level of a lateral condyle, which has a transverse main axis.

5.4 | Pterygoid

A very incomplete left pterygoid is preserved. It lacks the ectopterygoid ramus, and most of the palatine and quadrate rami, and is represented only by their bases (Figure 4; Table 1). The base of the quadrate ramus is transversely constricted in dorsal view, with concave lateral and medial margins. In lateral view, the quadrate ramus is dorsally oriented and forms a nearly straight angle with respect to the palatine ramus, a feature also shared with the holotype of *L. admixtus* (PULR 01). The dorsal surface of the quadrate ramus possesses a well-defined groove that narrows posteriorly and represents the probable osseous correlate of a cartilage attachment (Klembara & Welman, 2009), as occurs in other dinosauriforms (e.g., *Silesaurus opolensis*: ZPAL Ab III/361/41; *L. admixtus*: Ezcurra, Nesbitt, Fiorelli, et al., 2020). There is a small and ventrally projected process, which represents the base of the lip that medially delimits the basal articulation. This articulation received the basipterygoid process of the parabasisphenoid and is concave, facing dorsally to dorsomedially. The quadrate ramus is thin and its broken portion reveals a sigmoid (laterally concave and medially convex on its anterior surface) cross-section. The base of the ectopterygoid ramus is crescent-shaped, ventrally concave in cross-section. The area of the palatal ramus that, in the holotype of *L. admixtus* (Bittencourt et al., 2014), possesses a knob-like ventral projection immediately anterior to the basal articulation is not preserved.

5.5 | Vertebral column

Cervical and dorsal vertebrae are preserved in PULR V-111 (Figures 5 and 6; Tables 2–4). These vertebrae are slightly deformed because of transverse taphonomic compression. The neural spines are poorly preserved, and the centra are not fused to their respective neural arches, suggesting that the individual had not reached skeletal maturity (but see Griffin et al., 2020).

All the centra lack pneumatic foramina, but a conspicuous elliptical depression exists on the lateral surface of the first three preserved cervical vertebrae. Also interesting is the presence, in the same set of elements, of excavations around the diapophyses that become deeper and wider in more posterior neck vertebrae. The development of such excavations accompanies the increasing elevation and outward projection of the diapophyses. The

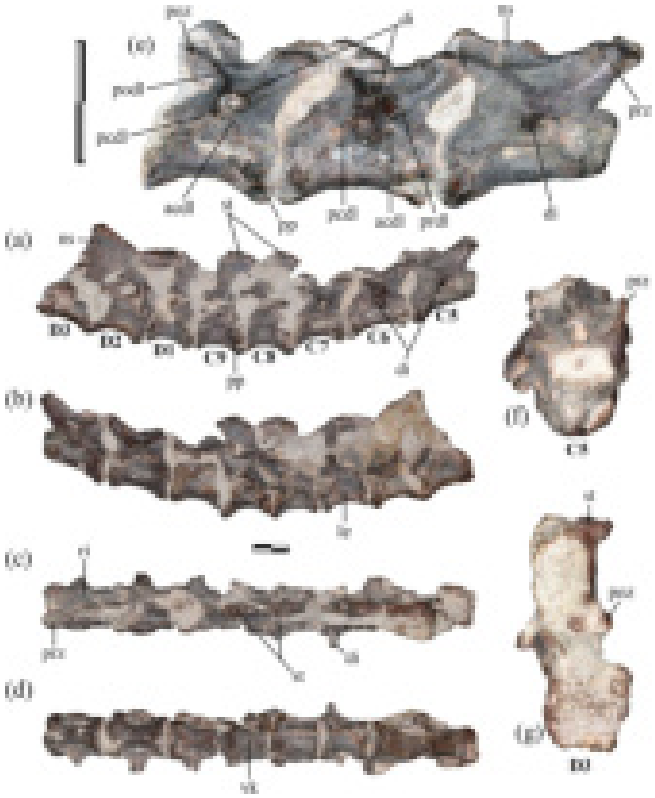

FIGURE 5 Posterior cervical and anterior dorsal vertebrae of *Lewisuchus admixtus* (PULR V-111) in: (a), right lateral; (b), left lateral; (c), dorsal and (d) ventral view; (e) detailed view of cervical vertebrae 5, 6, and 7 in right lateral view; (f), C5 in anterior view and (g), D3 in posterior view. References: acdl, anterior centrodiapophyseal lamina; pcdl, posterior centrodiapophyseal lamina; di, diapophysis; le, lateral excavation of centrum; ns, neural spine; podl, postzygodiapophyseal lamina; poz, postzygapophysis, pp, parapophysis; prdl, prezygodiapophyseal lamina; prz, prezygapophysis; ri, ridge; st, spine table; vk, ventral keel. Scale bars: 1 cm

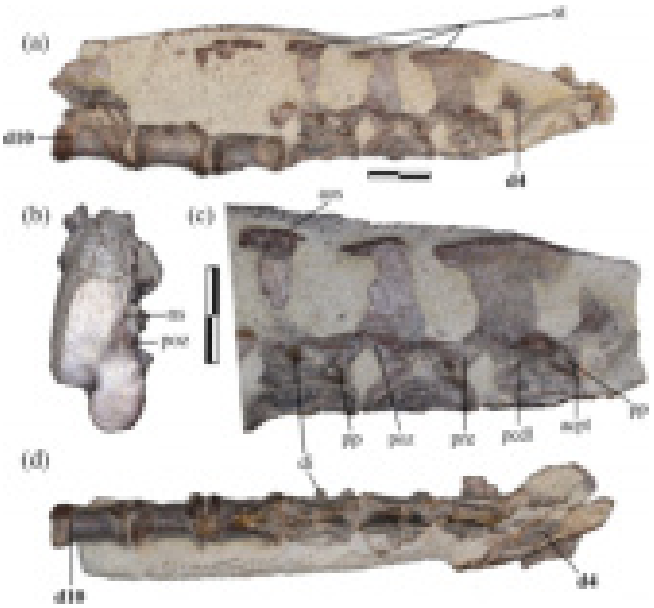

FIGURE 6 Middle and posterior dorsal vertebrae (d4–d10) of *Lewisuchus admixtus* (PULR V-111) in: (a), right lateral; (b), d10 in posterior view; (c), detailed view of dorsal vertebrae 4–7 in right lateral view; and (d), d4–d10 in ventral view. References: acpl, anterior centroparapophyseal lamina; aos, osteoderm; (d), dorsal vertebra; di, diapophysis; ns, neural spine; pcdl, posterior centrodiapophyseal lamina; poz, postzygapophysis; pp, parapophysis; prz, prezygapophysis; st, spine table Scale bar: 1 cm

TABLE 2 Measurements (in mm) of the cervical vertebrae of *Lewisuchus admixtus* (PULR V-111)

	Cv5	Cv6	Cv7	Cv8	Cv9
Centrum length	13.6	11.8	10.4	9.2	9.2
Anterior centrum height	(5.9)	6.4	6.4	6.4	6.7
Anterior centrum width	(5.7)	7.3	(7.5)	(6.1)	9.5
Posterior centrum height	6.6	6.2	5.8	5.5	6.3
Posterior centrum width	7.6	7.9	5.8	7.9	7.7
Length across zygapophyses	18.2	(11.0)	13.6	11.1	(7.4)
Maximum height	(14.0)	(13.5)	(14.1)	20.0	19.8

Note: Values between brackets indicate incomplete measurements (due to postmortem damage) and the value given is the maximum measurable. Maximum deviation of the calliper is 0.02 mm but measurements were rounded to the nearest 0.1 mm.

excavations present in the cervical centra and neural arches are similar to those frequently described for saurischian dinosaurs (Bonaparte, 1999; Colbert, 1970; Yates, Wedel, & Bonnan, 2012).

5.6 | Cervical vertebrae

The most anterior preserved vertebra of PULR V-111 is interpreted as the fifth cervical vertebra because of its matching morphology with that element in the articulated cervical series of the holotype of *L. admixtus* (PULR 01). Both vertebrae share a relatively elongated and parallelogram-shaped centrum in lateral view and a low and thick postzygodiapophyseal lamina in the neural arch. Bittencourt et al. (2014) interpreted that the cervical series of the holotype of *L. admixtus* was composed of seven vertebrae because there is a conspicuous morphological difference in the elongation of the centrum and the placement of the posterior articular surface in vertebrae anterior to the eighth presacral (a similar criterion

TABLE 3 Measurements (in mm) of the first to sixth dorsal vertebrae of *Lewisuchus admixtus* (PULR V-111), the fourth dorsal vertebra was not measured because it is extremely fragmentary

	D1	D2	D3	D5	D6
Centrum length	8.9	10.6	(10.5)	12.2	11.2
Anterior centrum height	7.1	6.9	–	–	–
Anterior centrum width	8.3	7.4	–	–	–
Posterior centrum height	6.0	7.8	(5.9)	–	–
Posterior centrum width	7.7	–	8.0	–	–
Length across zygapophyses	–	(8.6)	(10.7)	11.7	12.0
Maximum height	(17.9)	(20.6)	20.8	(16.7)	(17.7)

Note: Values between brackets indicate incomplete measurements (due to postmortem damage) and the value given is the maximum measurable. Maximum deviation of the calliper is 0.02 mm but measurements were rounded to the nearest 0.1 mm.

TABLE 4 Measurements (in mm) of the seventh to tenth dorsal vertebrae of *Lewisuchus admixtus* (PULR V-111)

	D7	D8	D9	D10
Centrum length	11.4	11.9	11.7	12.0
Anterior centrum height	—	(5.3)	6.8	7.2
Anterior centrum width	—	8.1	7.4	7.1
Posterior centrum height	—	(6.2)	7.4	6.9
Posterior centrum width	—	7.3	7.3	7.0
Length across zygapophyses	(12.7)	—	—	—
Maximum height	(19.7)	(21.0)	—	(17.0)

Note: Values between brackets indicate incomplete measurements (due to postmortem damage) and the value given is the maximum measurable. Maximum deviation of the calliper is 0.02 mm but measurements were rounded to the nearest 0.1 mm.

has been used by Piechowski & Dzik, 2010 for *S. opolensis*). We also recognize this morphological difference between the third and fourth preserved elements of PULR V-111 (here interpreted as the seventh and eighth presacral vertebrae). However, we prefer to consider the placement of the parapophyses exclusively in the centrum as a better landmark to distinguish between cervical and dorsal vertebrae. This is because, vertebral centrum shape and neural arch morphology, as will be detailed in the following description, are highly variable in shape and size along the vertebral column. Rib shape perhaps represents a better proxy to delimitate cervical and dorsal series; however, ribs are usually not preserved, especially in articulation. In this way, we recognize that parapophysis shape and position are the most useful anatomical sources to recognize vertebral positions in early dinosauromorphs.

As a result, we interpret that PULR V-111 possessed nine cervical vertebrae because in the tenth presacral vertebra (sixth as preserved) the parapophyses are positioned in the boundary between the centrum and neural arch. This observation is in agreement with the description of Bittencourt et al. (2014) that the ribs articulate with the centrum up to the tenth presacral vertebra in PULR 01.

5.7 | Cervical vertebra 5

This is the most elongated vertebra of the preserved series. The height of the posterior surface of the centrum represents one third of its total length. The anterior end of the centrum is damaged and, as a consequence, it is not possible to describe the morphology of the anterior articular surface. Nevertheless, it seems that the centrum was parallelogram-shaped in lateral view, with the anterior articular surface more dorsally positioned than the posterior one, as occurs in the anterior and middle postaxial cervical vertebrae of the holotype of *L. admixtus* (PULR 01) and in other early dinosauriforms (e.g., *L. talampayensis*: PVL 3870; *Asilisaurus kongwe*: Nesbitt, Langer, & Ezcurra, 2020). The ventral surface of the centrum is slightly concave in lateral view and has a faint longitudinal keel, but it is possible that its poor development is an artifact. The centrum is moderately compressed transversely around mid-length. Its lateral surface is excavated by an elliptical, anteroposteriorly elongated, and well-defined fossa that extends dorsally close to the level of suture between the centrum and neural arch. The parapophysis is preserved on the left side, being sub-circular in outline and slightly raised from the rest of the centrum. It is placed approximately at mid-height on the centrum and, although the area is damaged, it is clear that it was not adjacent to the anterior margin of the bone. The neural canal is transversely wider than tall in anterior view.

The neural arch has very low and thick prezygodiapophyseal and postzygodiapophyseal laminae, and very short anterior and posterior centrodiapophyseal laminae. By contrast, the fifth cervical vertebra of *S. opolensis* has well-developed lateral laminae (Piechowski & Dzik, 2010). The lateral surface of the neural arch posteriorly to the base of the diapophysis is shallowly excavated by a postzygapophyseal-centrodiapophyseal fossa. The surface of the bone anteriorly to the diapophysis is damaged and the morphology of the prezygapophyseal-centrodiapophyseal fossa cannot be determined. The centrodiapophyseal fossa is distinctly

smaller and deeper. A distinct, sharp ridge extends posteriorly from the base of the prezygapophysis but it does not reach the postzygapophysis. This ridge separates the base of the neural spine from the lateral surface immediately dorsal to the diapophysis. A thick and well-defined ridge connects the prezygapophysis with the anterior margin of the base of the neural spine, but it does not extend onto the anterior surface of the neural spine. Only the base of the diapophysis is preserved, which is relatively wide anteroposteriorly and sub-triangular in cross-section. Its main axis slants slightly anteroventrally in lateral view and is positioned immediately dorsal to the base of the neural arch.

The prezygapophysis is anterodorsally oriented and projects anteriorly beyond the anterior margin of the centrum. Its articular facet is sub-oval, with an anterolaterally-to-posteromedially oriented main axis, and faces dorsomedially. The postzygapophysis projects posteriorly at approximately the same level as the posterior edge of the centrum and apparently lacks an epipophysis. There seems to be a shallow depression immediately lateral to the base of the neural spine, but its depth seems to be exaggerated by bone collapse on the right side (the left side of the vertebra is damaged in this area). Only the base of the neural spine is preserved. It is laminar and extends anteroposterioly along the posterior two-thirds of the neural arch. The prespinal fossa is deep, subcircular, and its floor is formed by a transverse lamina that connects the base of the prezygapophyses.

5.8 | Cervical vertebra 6

This element is very similar in general aspect to the fifth cervical vertebra. The right diapophysis lacks its distal tip, and only the bases of the left diapophysis and of the neural spine are preserved. The postzygapophyses are completely lost. The vertebral centrum is sub-rectangular in lateral view, with the anterior articular surface positioned only slightly dorsal to the posterior one, contrasting with the more parallelogram-shaped centrum of the fifth cervical element. The lateral excavation is deep and well-defined, similar to the condition of the preceding vertebra. The centrum possesses a very low, longitudinal keel that extends along the preserved ventral surface of the bone. In sharp difference with the fifth cervical vertebra, the sixth element has well-developed and sharp anterior and posterior centrodiapophyseal, prezygodiapophyseal, and postzygodiapophyseal laminae, resembling the condition in the sixth cervical vertebra of *S. opolensis* (Piechowski & Dzik, 2010). The prezygapophyseal-centrodiapophyseal and postzygapophyseal-centrodiapophyseal fossae are deep and subtriangular, whereas the centrodiapophyseal fossa is also deep, but smaller. In congruence with the better developed laminae, the fossae on the neural arch are all deeper than in the fifth cervical vertebra. The prezygapophysis is slightly lower dorsoventrally than in the fifth cervical vertebra, but it also extends anteriorly beyond the anterior margin of the centrum. The diapophysis is lateroventrally oriented and trapezoidal or subtriangular in dorsal view, with a wider base. The main axis of the base of the diapophysis is anteroventrally to posterodorosally oriented. There is an incipient depression positioned immediately lateral to the base of the neural spine. The preserved morphology of the prespinal fossa and neural spine is consistent with those of the fifth cervical vertebra.

5.9 | Cervical vertebra 7

This element differs from the previously described cervical vertebrae in being proportionally anteroposteriorly shorter, with the length of the centrum approximately two thirds that of the preceding element. The left surface of the seventh cervical vertebra is strongly damaged and the neural spine is almost completely lost. The anterior articular surface of the centrum is positioned slightly dorsal to the posterior one in lateral view, resembling the condition of the sixth cervical vertebra. The prezygapophyseal-centrodiapophyseal and postzygapophyseal-centrodiapophyseal fossae are deeper and broader than in more anterior cervical vertebrae. The postzygodiapophyseal lamina is more arched posteriorly and the prezygapophysis more dorsally oriented than in the preceding cervical vertebrae. The postzygapophysis lacks an epipophysis. The base of the neural spine indicates that it was anterodorsally oriented in lateral view, as occurs in the holotype of *L. admixtus* (PULR 01; Bittencourt et al., 2014) and in middle-posterior cervical vertebrae of *A. kongwe* (Nesbitt et al., 2020).

5.10 | Cervical vertebra 8

The gross morphology and proportions of this element resemble those of the seventh cervical vertebra (Figure 6), but differs in the presence of a proportionally shorter centrum, with less excavated lateral surfaces, and anterior and posterior articular surfaces positioned at approximately the same level in lateral view. The ventral surface of the centrum possesses a faint longitudinal keel, resembling more anterior cervical vertebrae. The prezygapophysis is more dorsally oriented, the diapophysis slightly more anteriorly placed, and the fossae delimited by the diapophysis and its associated

laminae are deeper than in the preceding cervical vertebrae. The postzygapophysis lacks an epipophysis.

The neural spine is completely preserved and distinctly tall, that is, approximately as tall as the rest of the vertebra. It is anterodorsally oriented in angle of approximately 30° to the vertical axis, resembling the condition in a middle-posterior cervical vertebra of *A. kongwe* (Nesbitt et al., 2020). The anterior margin of the neural spine is more slanted than the posterior one, thus forming a fan-shaped structure in lateral view, resembling the condition in the eighth presacral vertebra of the holotype of *L. admixtus* (PULR 01). The distal end of the neural spine is transversely thickened, forming a spine table and giving the neural spine a "T"-shaped profile in anterior or posterior views. The distal surface of the neural spine is transversely convex and possesses a rugose surface that contrasts with the smooth surface of the rest of the neural spine.

5.11 | Cervical vertebra 9

This vertebra is very similar in morphology to the preceding one, but it is slightly anteroposteriorly shorter and lacks the faint longitudinal ridge on the ventral surface of the centrum. The laminae, fossae, and apophyses are severely damaged. However, it seems that the anterior centrodiapophyseal lamina contacts the parapophysis, thus forming a paradiapophyseal lamina. The parapophyses, which are damaged in more anterior cervical vertebrae, are laterally raised on a short stalk and their articular surfaces are flat, sub-oval, and dorsoventrally higher than long. The neural spine possesses the same morphology as that described for the eighth cervical vertebra.

5.12 | Dorsal vertebrae

The dorsal vertebrae of PULR V-111 are currently preserved in two blocks. The first block preserves the first three dorsal vertebrae in articulation with the cervical vertebrae, and the second block preserves the fourth to tenth dorsal vertebrae in articulation. In spite of the poor preservation, there is no evidence of the presence of hyposphene and hypantrum articulations along the dorsal column.

5.13 | Dorsal vertebra 1

This element is very similar to the last two cervical vertebrae and, in particular, it resembles the ninth cervical vertebra in the absence of a ventral keel on the centrum. Yet, as mentioned above, it differs in having the parapophysis positioned partially on the neural arch. The vertebra is severely damaged, precluding a detailed description, but it preserves a complete left diapophysis, contrasting with more anterior elements. The diapophysis is laterally oriented and is transversely shorter than the centrum. The centrodiapophyseal fossa slightly excavates the base of the diapophysis, thus being shallower than in more anterior vertebrae.

5.14 | Dorsal vertebra 2

The second dorsal vertebra lacks the posterolateral corners of the centrum, the zygapophyses (except for the left prezygapophysis preserved in sagittal section), the left diapophysis, and the distal end of the right diapophysis. The neural spine is broken in two pieces, displaced from one another. The preserved morphology of this vertebra is congruent with that of the two preceding elements, with the exception that the parapophysis is completely within the anteroventral corner of the neural arch and the distal end of the neural spine is anteroposteriorly longer.

5.15 | Dorsal vertebra 3

The anterior and posterior margins of the centrum are damaged, and the right base of the neural arch and both postzygapophyses are not preserved. The centrum possesses a similar morphology to those of the four preceding vertebrae, with a transversely convex and smooth ventral surface and a shallowly excavated lateral surface. Although damaged, it can be observed that the posterior end of the centrum is sub-oval in posterior view, transversely broader than tall. The diapophysis is positioned on the anterior third of the base of the neural arch, as occurs in the last two cervical vertebrae and more anterior dorsal vertebrae, and the paradiapophyseal lamina is well developed and anteroventrally oriented. The other laminae of the neural arch are not preserved. The anterior margin of the neural spine is anterodorsally oriented forming an angle of around 30° to the vertical axis in lateral view. However, its posterior margin is almost vertical, resulting in an asymmetrically fan-shaped neural spine in lateral view, closely resembling the condition in the last two cervical vertebrae. The ventral half of the anterior margin of the neural spine is anteriorly concave in lateral view, whereas the posterior margin is straight. The neural spine of this vertebra (and apparently also that of the second dorsal vertebra) is anteroposteriorly longer than those of more posterior dorsal vertebrae. Given their orientation and anteroposterior development,

it seems that the distal ends of the neural spines of, at least, the second and third dorsal vertebrae contacted one another. This condition also occurs between the fourth and fifth dorsal vertebrae of the holotype of *L. admixtus* (Bittencourt et al., 2014) and in the anterior-middle dorsal vertebrae of *L. talampayensis* (Sereno & Arcucci, 1994). The spine table is more transversely expanded toward the posterior end of the neural spine, resulting in a subtriangular outline in dorsal view. The distal surface of the neural spine is incipiently transversely convex.

5.16 | Dorsal vertebra 4

This vertebra is very incomplete and only its short, posterolaterally oriented right postzygapophysis is well preserved.

5.17 | Dorsal vertebra 5

This vertebra preserves the neural arch and the dorsal portion of the centrum. The bases of the diapophyses are preserved and the right one is better exposed (Figure 6). The parapophysis and diapophysis are positioned in the same process and very close to one another, but still distinctly separated. The articular facet of the parapophysis is suboval, with an anteroventrally to posterodorsally oriented main axis. The diapophysis is mainly laterally oriented, but also faces slightly dorsally. The paradiapophyseal lamina is very short, because of the close proximity between parapophysis and diapophysis. A short anterior centroparapophyseal lamina projects from the parapophysis anteroventrally and merges abruptly with the anteroventral corner of the neural arch. The posterior centrodiapophyseal lamina is distinctly shorter than those of the cervical and more anterior dorsal vertebrae. The prezygodiapophyseal lamina is sharp and very short. The postzygodiapophyseal lamina is short, subhorizontally oriented, and incipiently reaches the postzygapophysis. The prezygapophyseal-centrodiapophyseal fossa is moderately deep, but small and mainly anteriorly facing. The centrodiapophyseal fossa is as deep as the latter, but distinctly larger. The postzygapophyseal-centrodiapophyseal fossa is the shallowest, contrasting with the condition in preceding vertebrae, and opens posterolaterally. The prezygapophysis and postzygapophysis are relatively short and sub-horizontally oriented. The prezygapophysis does not project anteriorly beyond the level of the anterior margin of the centrum, whereas the postzygapophysis extends beyond the posterior margin of the centrum in lateral view.

The anterior and posterior margins of the neural spine are damaged, but it is clear that the spine was trapezoidal in lateral view, expanding anteroposteriorly toward its distal end. Indeed, the distal end of the neural spine is anteroposteriorly longer than the length across the zygapophyses, as occurs in at least one posterior dorsal vertebra of the holotype of *L. talampayensis* (PULR 09). Similarly, anteroposteriorly expanded neural spines, but not exceeding the length across zygapophyses, have also been reported in the holotype of *L. admixtus* (Bittencourt et al., 2014) and on other dorsal vertebrae of *L. talampayensis* (Sereno & Arcucci, 1994). The neural spine of PULR V-111 is asymmetric in lateral view, more expanded posteriorly than anteriorly. Its main axis is vertical, contrasting with the anterodorsally oriented neural spines of the posterior cervical and anterior dorsal vertebrae. The spine table is well-developed and maintains a constant transverse width through its anteroposterior length, contrasting with the transverse expansion toward the posterior end present in the second and third dorsal vertebrae.

5.18 | Dorsal vertebrae 6 and 7

Both vertebrae are partially preserved, missing most of the centra, transverse processes, and neural spine margins. Their preserved overall morphology resembles that of the fifth dorsal vertebra. The centra are transversely compressed around mid-length. The zygapophyses are relatively short and sub-horizontal. It cannot be determined if the neural spines were anteroposteriorly expanded toward their distal end. The spine tables are as developed as in the preceding vertebrae of the series, but are nearly smooth dorsally, with a gently rough surface.

5.19 | Dorsal vertebra 8

This vertebra preserves most of its centrum (missing its anteroventral third), but the neural arch preserves only the distal margin of the neural spine and the right prezygapophysis. The centrum is transversely compressed around mid-length and the lateral surface lacks a fossa. The spine table is as developed as those of the preceding three dorsal vertebrae.

5.20 | Dorsal vertebra 9

This vertebra is represented by a complete centrum. As in other middle dorsal vertebrae, the centrum is elongated, approximately duplicating its height, and

the concave lateral surface lacks a fossa. The ventral surface is transversely convex and smooth, without a groove or keel. The anterodorsal corner of the centrum preserves the distal tip of the anterior centrodiapophyseal lamina.

5.21 | Dorsal vertebra 10

The centrum of this vertebra is completely exposed, but the neural arch is covered with matrix on the left side. The centrum is complete and the neural arch lacks most of the transverse processes, most of the prezygapophyses, the tip of the postzygapophyses, and the distal end of the neural spine. The centrum is anteroposteriorly elongated, with morphology and proportions consistent with those of the preceding vertebra. In the neural arch, the anterior centrodiapophyseal lamina is sharp and reaches the anteroventral corner of the arch. Damage in the area of the posterior centrodiapophyseal lamina precludes determining if it is very short or absent. The prezygapophyseal and postzygapophyseal laminae are absent. The postspinal fossa invades dorsally only the base of the neural spine and separates the postzygapophyses from one another.

5.22 | Dorsal ribs

The proximal end of the left rib of the second dorsal vertebra is preserved. The rib is dichocephalous, with a large and narrow capitulum. The tuberculum is relatively short and robust. Both processes are separated by a posteriorly facing, subtriangular depression. The shaft is subtriangular in cross-section, with a ridge that forms an anterior apex extending longitudinally from the base of the capitulum toward the distal end of the element. Other dorsal ribs are represented by fragments of disarticulated and poorly preserved shafts.

5.23 | Gastralia

Two pairs of gastralia are preserved in PULR V-111 and in approximate natural position to one another (Figure 1). The longest gastral element has a maximum preserved length of 19.9 mm. These rod-like bones show that the preserved region of the gastral basket—it cannot be determined which region is preserved—has well anteroposteriorly separated gastralia that form an angle of approximately 110° to one another. The gastral elements have a sub-oval cross-section, dorsoventrally taller than anteroposteriorly deep.

5.24 | Sacrum

Both sacral vertebrae and ribs articulated with the left ilium are preserved in PULR V-113 (Figure 7; Table 5). The sacrum is composed of two unfused vertebrae, but each being fused with their respective ribs. The vertebral centra are spool-shaped in ventral view, transversely and ventrally expanded at their anterior and posterior ends. Their ventral surfaces are transversely convex and smooth, without a keel or groove. The second sacral centrum is longer than the first, and also has a wider posterior end. The first sacral rib is attached to the anterior half of the centrum and to the base of the neural arch, whereas the second sacral rib articulates around the midlength of the centrum. The ribs are not shared between both sacral vertebrae, but the base of the first sacral rib projects slightly anteriorly beyond the anterior rim of the centrum, indicating that a very small portion of it

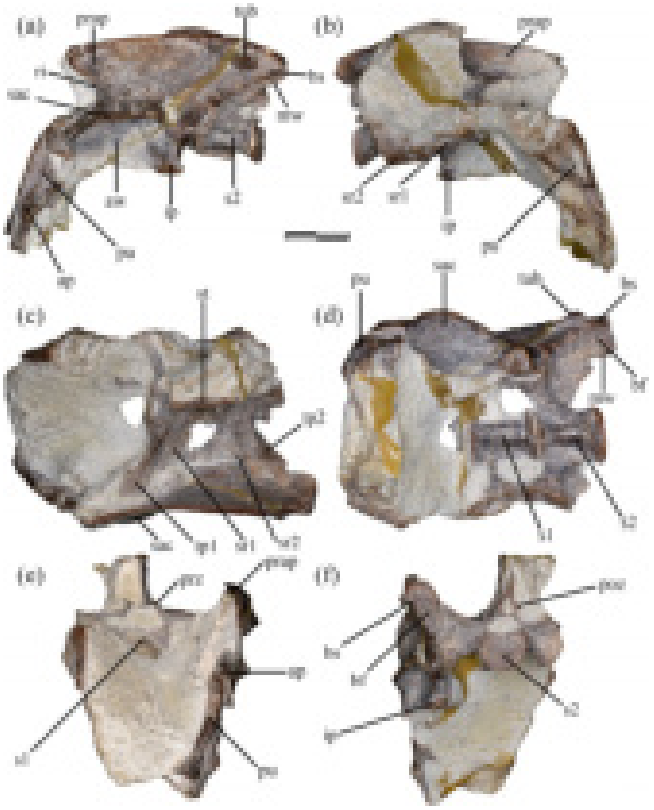

FIGURE 7 Articulated pelvic girdle and sacrum of *Lewisuchus admixtus* (PULR V-113) in: (a), left lateral; (b), right lateral; (c), dorsal; (d), ventral; (e), anterior, and (f), posterior views. References: ap, ambiens process; aw, acetabular wall; bf, brevis fossa; bs, brevis shelf; ip, ischiadic peduncle; mw, medial wall of brevis shelf; poz, postzygapophysis; prap, preacetabular process; prz, prezygapophysis; pu, pubis; ri, ridge; S1, sacral 1; S2, sacral 2; sac, supraacetabular crest; sr1, sacral rib 1; sr2, sacral rib 2; st spine table; tp1, transverse process of sacral 1; tp2, transverse process of sacral 2; tub, tuberosity on postacetabular process. Scale bar: 1 cm

TABLE 5 Measurements (in mm) of sacral vertebrae and ribs of *Lewisuchus admixtus* (PULR V-113)

	S1	S2
Centrum length	8.9	9.4
Anterior centrum height	6.2	—
Anterior centrum width	8.5	6.6
Posterior centrum height	—	6.8
Posterior centrum width	7.0	7.9
Length across zygapophyses	10.5	(12.0)
Maximum height of vertebra	20.2	(16.1)
Maximum width of centrum + rib	21.4	20.1
Depth of articular facet for ilium	8.0	7.9

Note: Values between brackets indicate incomplete measurements (due to postmortem damage) and the value given is the maximum measurable. Maximum deviation of the calliper is 0.02 mm but measurements were rounded to the nearest 0.1 mm.

articulated with the posterodorsal corners of the last dorsal centrum.

The first sacral vertebra and ribs are fairly complete. Only the anterior surface of the centrum is damaged and the right rib lacks its lateral end. The right side of the base of the neural arch is covered with matrix. The centrum and neural canal are transversely wider than dorsoventrally tall. The prezygapophysis is very short and anterolaterally oriented, projecting slightly beyond the level of the anterior margin of the centrum. Its articular facet is considerably smaller than those of the presacral vertebrae. The postzygapophysis is similarly short and does not project beyond the level of the posterior rim of the centrum. The neural spine is taller than anteroposteriorly long and laminar in cross-section. The base of the neural spine possesses an elongated depression with an anterolateral to posteromedial long axis. The neural spine expands anteroposteriorly toward its distal end, resulting in a fan-shaped structure in lateral view, slightly more posteriorly than anteriorly expanded. The distal margin of the neural spine is convex in lateral view and slightly thickened transversely, but clearly not as much as in the dorsal vertebrae.

The first sacral rib is lateroventrally oriented, but it does not project ventrally beyond the ventral margin of the vertebral centrum. The rib expands anteroposteriorly toward its distal end, which is composed of two regions. The posterolateral end of the rib is dorsoventrally thick and finishes in a facet for the articulation of the ilium. This facet is subrectangular and very slightly ventrally oriented, with an anterodorsally to posteroventrally oriented main axis. It articulates with the ilium at the level of the base of the iliac blade, with its anterior margin slightly posterior to the base of the preacetabular process and the posterior margin reaching the level of the posterior edge of the base of the ischiadic peduncle. The anterolateral corner of the rib is formed by a dorsoventrally laminar process that projects anterolaterally and has a constriction around mid-length in dorsal view. This process is dorsal to the articular facet for the ilium and finishes before contacting the preacetabular process of that bone.

The second sacral vertebra lacks most of the neural spine, and its right rib lacks its posterolateral corner. The right side of the neural arch is covered with matrix. The posterior articular surface of the centrum is slightly concave and has a kidney-shaped contour, as the result of a concave dorsal margin. The preserved morphology of the neural arch is congruent with that of the first sacral vertebra. The postzygapophysis is short, not reaching the level of the posterior rim of the centrum, and its articular facet is small, sub-oval and lateroventrally faced. There is no hyposphene. The limit between the vertebra and the sacral ribs is still discernible in ventral view as a rounded and thick lip.

The second sacral rib is slightly less laterally extended than the first and has an anteroposterior constriction close to its base. The distal end of the rib is strongly anteroposteriorly expanded and is subdivided into two distinct structures. The anterolateral corner includes the articular facet for the ilium and also articulates anteriorly with the first sacral rib. Thus, the first and second sacral ribs form together a continuous articular surface, which is anteroposteriorly concave in dorsal view. The iliac articular surface of the second sacral rib is L-shaped in lateral view, with an anteroposterior main axis and a short dorsal process. This rib articulates with the anterior third of the postacetabular process, adjacent to its ventral margin. The posterolateral corner of the rib is formed by a flange-like process dorsal to the articular facet for the ilium, as occurs in aphanosaurs, silesaurids, and early dinosaurs (Nesbitt et al., 2017). This process sits on the dorsal surface of the medial longitudinal shelf of the postacetabular process of the ilium (i.e., the flange of bone that forms the medial border of the posterior portion of the brevis fossa). The distal end of the posterolateral process of the sacral rib is forked by a deep notch, contrasting with the undivided process present in other known avemetatarsalians (e.g., *L. talampayensis*; Bonaparte, 1975; *Herrerasaurus ischigualastensis*; Novas, 1994; *S. opolensis*; Dzik, 2003), and it finishes 1 cm before reaching the posterior margin of the postacetabular process.

5.25 | Ilium

PULR V-111 preserves an almost complete left ilium, missing most of the anterior two-thirds of the dorsal

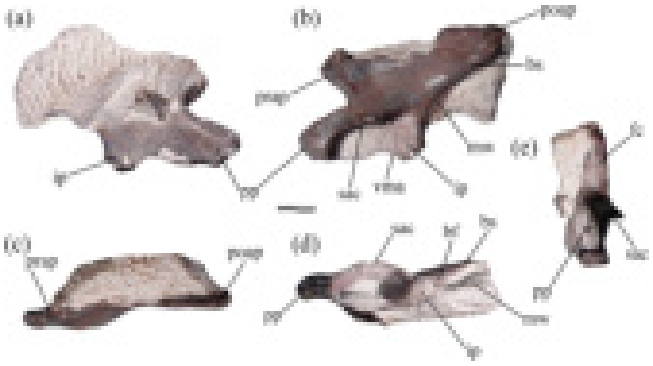

FIGURE 8 Left ilium of *Lewisuchus admixtus* (PULR V-111) in: (a), medial; (b), lateral; (c), dorsal; (d), ventral; and (e), anterior views. References: bf, brevis fossa; bs, brevis shelf; fc, fossa cuppedicus; mw, medial wall of brevis fossa; ip, ischiadic peduncle; poap, postacetabular process; pp, pubic peduncle; pre, preacetabular process; sac, supraacetabular crest; vma, ventral margin of acetabular wall. Scale bar: 1 cm

margin of the blade and part of the ventral margin of the acetabular wall (Figure 8; Table 6). PULR V-113 preserves a complete left ilium, which probably lacks the ventralmost margin of the acetabular wall (Figure 7; Table 7).

The lateral surface of the iliac blade is anteroposteriorly concave and possesses multiple striations parallel to one another on the preacetabular and postacetabular processes. The lateral surface of the preacetabular process is slightly convex and rugose adjacent to its dorsal margin, which may represent the site of origin of the *M. iliofemoralis cranialis*, as hypothesized for several other dinosauriforms (Carrano & Hutchinson, 2002; Langer, 2003). The striations of the postacetabular process are anteroventrally to posterodorsally oriented and indicate the origin of the *Mm. iliotibialis*, as occurs in crocodiles and dinosaurs (Carrano & Hutchinson, 2002). In PULR V-113, there is a thick ossification on the lateral surface of the postacetabular process ("tub" in Figure 7) that probably was also involved in the origin of the *iliotibialis* muscles. This ossification is absent in PULR V-111 and CRILAR-Pv 552 (see Ezcurra, Nesbitt, Fiorelli, et al., 2020) and this difference is here interpreted as intraspecific, as proposed for some early dinosaurs (Garcia, Pretto, Dias-Da-Silva, & Müller, 2019). The preacetabular process is relatively short, not surpassing the anterior tip of the pubic peduncle, and sub-triangular in lateral view, with an anteriorly oriented apex. The process is slightly laterally tilted in dorsal view with respect to the main axis of the acetabulum. The preacetabular process lacks the transverse expansion present in some early saurischians, such as *H. ischigualastensis* (Novas, 1994). The anteroventral margin of the preacetabular process is thickened and extends posteroventrally as a ridge that contacts the dorsal margin of the supraacetabular crest, as occurs in other early avemetatarsalians (Nesbitt et al., 2010, 2017). This ridge delimits laterally a transversely broad and shallow fossa that opens anteriorly. This fossa is subtriangular and shows an anterodorsally oriented apex, probably homologous to the cuppedicus fossa of averostran theropods, which constitutes the attachment site of *M. iliofemoralis internus* (Novas, 1996; Rowe, 1989).

The postacetabular process is distinctly longer than the preacetabular process and sub-triangular in lateral view, with the dorsal and ventral margins nearly straight and converging posterodorsally. The postacetabular process is also longer than the length of the acetabulum. The site of origin of the *M. caudofemoralis brevis* is represented by a shallow and transversely narrow fossa (i.e., brevis fossa) on the ventral surface of the posterior two-thirds of the postacetabular process. It is delimited laterally by a brevis shelf that is positioned only slightly dorsal to the ventromedial margin of the postacetabular process. As a result, the brevis fossa is only incipiently visible in lateral view. The lateral and medial margins of the fossa diverge posteriorly very slightly from one another and, as a consequence, the fossa acquires a trapezoidal profile in ventral view. The brevis shelf does not reach the level of the ischiadic peduncle. The ventromedial margin of the postacetabular process bears a longitudinal medial shelf ("mw" in Figures 7 and 8) and on its posterior portion sits the posterolateral process of the second sacral rib. This shelf extends from the base of the ischiadic peduncle to the end of the postacetabular process.

The pubic peduncle is anteroventrally oriented at an angle of 45° to the horizontal plane and has a strongly transversely convex pubic articular surface. This articular surface is oval in contour, with an anteroposterior main axis. The posterolateral margin of the pubic peduncle bears the anteroventral extension of the supraacetabular crest, but it fails to reach the articular surface for the pubis. The extension of this crest results in a subtriangular cross-section of the pubic peduncle, especially on its proximal portion. The supraacetabular crest is prominent and well-developed, with its lateralmost extension positioned immediately posterior to the base of the pubic peduncle. This crest is lateroventrally oriented and partially covers the acetabulum in lateral view, forming an extensive shelf. The anteroposterior length of the acetabulum is greater than its dorsoventral height. It is deeper on its posterior half, and nearly closed. Although the ventral margin of the acetabular wall is damaged, its posterior end is preserved in PULR V-111, showing the presence of a deeper ventral notch. As a

TABLE 6 Measurements (in mm) of the left pelvic girdle, femur and tibia of *Lewisuchus admixtus* (PULR V-111)

	Ilium	Pubis	Ischium	Femur	Tibia
Length	44.6	(59.2)	47.7	96.5	106.8
Pubic peduncle length	13.3	—	—	—	—
Pubic peduncle distal width	4.5	—	—	—	—
Pubic peduncle distal depth	8.8	—	—	—	—
Ischiadic peduncle length	9.7	—	—	—	—
Ischiadic peduncle distal width	5.6	—	—	—	—
Ischiadic peduncle distal depth	(7.1)	—	—	—	—
Acetabulum length	19.0	—	—	—	—
Iliac blade length	40.3	—	—	—	—
Iliac blade height	14.8	—	—	—	—
Preacetabular process length	5.4	—	—	—	—
Preacetabular process height at base	(10.3)	—	—	—	—
Postacetabular process length	16.1	—	—	—	—
Maximum height	28.6	—	—	—	—
Proximal width	—	—	5.5	7.5	11.6
Proximal depth	—	(11.6)	(19.0)	16.2	20.9
Distal width	—	—	—	13.1	7.4
Distal depth	—	—	—	14.7	10.9

Note: Values between brackets indicate incomplete measurements (due to postmortem damage) and the value given is the maximum measurable. Maximum deviation of the calliper is 0.02 mm but measurements were rounded to the nearest 0.1 mm. Width refers to transverse width and depth to anteroposterior depth.

TABLE 7 Measurements (in mm) of the pelvic girdle of *Lewisuchus admixtus* (PULR V-113)

	L ilium	R pubis	L pubis	R ischium	L ischium
Length	35.9	(22.8)	(20.7)	(22.7)	(12.2)
Pubic peduncle length	10.0	—	—	—	—
Pubic peduncle distal width	3.8	—	—	—	—
Pubic peduncle distal depth	6.6	—	—	—	—
Ischiadic peduncle length	5.5	—	—	—	—
Ischiadic peduncle distal width	4.0	—	—	—	—
Ischiadic peduncle distal depth	4.4	—	—	—	—
Acetabulum length	14.3	—	—	—	—
Iliac blade length	34.2	—	—	—	—
Iliac blade height	9.3	—	—	—	—
Preacetabular process length	5.4	—	—	—	—
Preacetabular process height at base	9.4	—	—	—	—
Postacetabular process length	13.9	—	—	—	—
Maximum height	22.2	—	—	—	—
Proximal width	—	—	2.5	3.2	3.8
Proximal depth	—	(7.7)	(7.0)	(10.0)	16.6

Note: Values between brackets indicate incomplete measurements (due to postmortem damage) and the value given is the maximum measurable. Maximum deviation of the calliper is 0.02 mm but measurements were rounded to the nearest 0.1 mm.
Abbreviations: L, left; R, right.

result, the acetabulum would be more open than in other nondinosaurian avemetatarsalians (Nesbitt et al., 2017). The medial surface of the acetabular wall is distinctly convex.

The ischiadic peduncle is proportionally large, transversely wide, and medially continuous with the medial margin of the acetabulum. Such condition resembles that of *Ixalerpeton polesinensis* (Cabreira et al., 2016), but differs from that of dinosaurs (e.g., *Panphagia protos* and *Buriolestes schultzi*) in which this peduncle is much more reduced and medially displaced. The lateral surface of the ischiadic peduncle and the posterior region of the acetabulum lacks a well-defined antitrochanter. This surface is flat, smooth, and should have articulated with the posteromedial surface of the femoral head. The ischiadic peduncle is shorter than the pubic peduncle and has a slightly concave posterior margin in lateral view. Its distal end is laterally expanded and houses the articular surface for the ischium, which faces ventrally and is slightly convex and subtriangular in profile, with a laterally oriented apex.

The articulations between the ilium and the two sacral ribs are exposed in PULR V-113 and positioned at the level of the supraacetabular crest. The articulation with the first sacral rib extends from the ventral half of the base of the preacetabular process to the mid-length of the acetabular wall, acquiring an anterodorsally to posteroventrally oriented main axis. The articulation for the second sacral rib extends from the posterodorsal corner of the acetabular wall, through the base of the ischiadic peduncle, and along the ventral edge of the postacetabular process. Its posterior end finishes well anterior to the posterior margin of the process. In lateral view, the posteroventral margin of ilium is convex immediately above the ischiadic peduncle. Such a convexity matches the curved posterior margin of the second sacral rib.

5.26 | Pubis

The left pubis of PULR V-111 lacks its distal portion and is exposed in lateral and anterior views (Figure 9; Table 6), whereas the proximal end of the left pubis of PULR V-113 is preserved and its medial surface is covered with matrix (Figure 7; Table 7). The pubis of the latter specimen is in natural articulation with the ilium, showing that the pelvis might have been mesopubic, with the pubis forming an angle of nearly 90° to the horizontal plane, a condition similar to that of *L. talampayensis* (Bonaparte, 1975). The anterior surface of the proximal end of the pubis is strongly transversely convex. The lateral surface is slightly depressed immediately below the iliac articulation. In the transition between the proximal body and the shaft, there is a prominent, mound-like

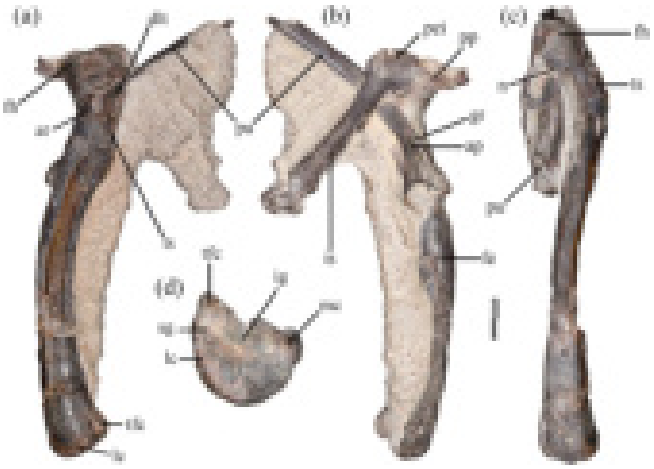

FIGURE 9 Left ischium, pubis, and femur of *Lewisuchus admixtus* (PULR V-111) in: (a), lateral view; (b), ischium in medial and pubis in lateral view, femur in posteromedial view; (c), anterior view; (d); close-up of femur in distal view. References: ap, ambiens process; dlt, dorsolateral trochanter; fe, femur; fh, femoral head; gr, groove; ig, intercondylar groove; is, ischium; lc, lateral condyle; mc, medial condyle; n, notch; pei, proximal end of ischium; pp, pubic peduncle; pu, pubis; sg, shallow groove; tfc, tibiofibular crest; ts, trochanterric shelf. Scale bar: a–c, 1 cm; D, 5 mm

tuberosity (i.e., pubic tubercle) that is anteriorly bounded by a longitudinal groove in both specimens. The tuberosity, groove, and convex area are finely striated in PULR V-111 and may have allowed the anchoring of *M. ambiens* (Hutchinson, 2001; Langer, 2003). In anterior view and distal to the pubic tubercle, a thin, anteroposteriorly compressed lamina of bone represents the proximal portion of the pubic apron.

On the posterior margin of the proximal end, proximal to the level of the *M. ambiens* attachment, the base of the pubo-ischiadic lamina is preserved as a ventromedially oriented thin flange. The preserved portion of this lamina does not allow determining the presence and shape of an obturator foramen. The lamina is separated from the rest of the bone by a very sharp and posteroproximally to anterodistally oriented change in slope.

The preserved portion of the pubic shaft is continuously arched anteriorly in lateral view. Only the base of the pubic apron is preserved along the shaft, forming a comma-shaped cross-section. The main axis of the pubic cross-section where it is broken off in PULR V-111 is rotated posteriorly approximately 10° with respect to that of the proximal surface of the bone.

5.27 | Ischium

PULR V-111 preserves a left ischium exposed in medial view (Figure 9; Table 6) and PULR V-113 preserves the

proximal end of the left ischium and about the same portion of the right one (Table 7). The three ischia reveal most of the bone anatomy, except for ventral edge of the shaft and most of the distal end. The ischium has a relatively transversely broad proximal end, which articulates with the ilium and the pubis, and a plate-like shaft. It is slightly shorter than half the length of the femur in PULR V-111.

The proximal end of the ischium is preserved in articulation with a fragment of the pubo-ischiatic plate of the pubis in PULR V-111, but it is not clear how far distally this contact extended. The proximal margin of the ischium is better preserved in the left bone of PULR V-111 and its posterior portion is composed of two continuous surfaces, which are smooth—but with faint, mostly transverse grooves—and slightly differentiated by an anteromedially to posterolaterally oriented change in slope. The more posterior surface is subtriangular and includes the dorsally oriented facet for articulation with the ilium. The more anterior surface forms the antitrochanter, which is subtriangular, transversely concave, and anteroposteriorly convex, as well as anteroposteriorly longer, transversely broader, and slightly more laterally oriented than the iliac surface. The articular surface for the pubis is separated from the others by a broad and laterally facing fossa, which thins the proximal margin of the bone to a sheet-like lamina. Anteriorly to this fossa, the proximal end of the ischium expands laterally and broadens again to house a D-shaped—as preserved—and mostly smooth pubic articular surface. The medial side of the proximal end of the bone is formed by two flat surfaces separated from one another by a longitudinal change of slope close to the level of contact between the iliac articular surface and the antitrochanteric surface. The pubic peduncle has a concave medial surface.

The preserved portion of the ischial shaft is plate-like and has a flat symphyseal facet that does not reach the dorsal edge of the bone. The ischium is laterally flexed at its proximal half and the rest of the shaft distal to this is straight in both anterior and posterior views. The shaft possesses a slight torsion of approximately 20° through its length, in which the inner surface of the shaft is dorsomedially oriented proximally and becomes strictly medially facing distally. The posterodorsal surface of the ischium has a longitudinal groove that excavates at least the proximal half of the shaft. This groove is well delimited medially by a thin dorsally directed flange and, as a result, the groove is visible in both lateral and dorsal views. A dorsomedial low tuberosity extends along the distal half of the medial surface of the shaft dorsal to the symphyseal region. The distal end of the bone is not expanded transversely and the preserved portion of the distal margin is straight and posterodorsally to anteroventrally oriented in lateral view.

5.28 | Femur

The left femur is preserved in both PULR V-111 and PULR V-113. The latter specimen preserves approximately the proximal fourth of the bone (Table 8), whereas the other femur is fairly complete, missing only the anterolateral surface of most of its shaft (Figure 9; Table 6). This bone is also transversely compressed and its posteromedial surface is covered with matrix. The femur of PULR V-111 is 89.4% larger than that of PULR V-113, as estimated based on the lengths of the main axis of the proximal ends. The femora have a consistent morphology and the description is mainly based on PULR V-111.

The femur has a distinct sigmoid profile lateral view, arching posteriorly at the proximal half and anteriorly distal to that. The shaft is also sigmoid in anterior view due to a medial inflexion of the proximal portion and a slight medial arching around mid-length. The femoral head is sub-oval in proximal view and its surface is decorated by rugosities and striations that suggest the presence of a cartilaginous cap (see Tsai & Holliday, 2015). The proximal surface of the bone lacks the well-defined longitudinal groove present in *A. kongwe*, more deeply nested silesaurids, and several early dinosaurs (Dzik, 2003; Ezcurra, 2006; Nesbitt, 2011; Nesbitt et al., 2010). In PULR V-113, the lateral tuber (sensu Nesbitt, 2011) forms an obtuse angle between the nearly straight anterior and anterolateral margins of the femoral head in proximal view. The posteromedial margin of the femoral head bears a medially projected anteromedial tuber and a well-developed posteromedial tuber. Between the latter and the posterolateral tip of the articulation, the margin of the femoral head is not angled as in most silesaurids (Dzik, 2003; Ezcurra, 2006), but excavated by a subtle facies articularis antitrochanterica.

TABLE 8 Measurements (in mm) of the left femur and right tibia of *Lewisuchus admixtus* (PULR V-113)

	Femur	Tibia
Length	(30.0)	(34.9)
Proximal width	14.4	8.1
Proximal depth	7.0	17.6

Note: Values between brackets indicate incomplete measurements (due to postmortem damage) and the value given is the maximum measurable. Maximum deviation of the calliper is 0.02 mm but measurements were rounded to the nearest 0.1 mm.

The femoral head has a poorly developed anteromedial projection with a somewhat flattened medial margin. The femoral head is differentiated from the shaft by an anteromedial notch that resembles that of the *Lewsisuchus admixtus* specimen CRILAR-Pv 552 (Ezcurra, Nesbitt, Fiorelli, et al., 2020), *A. kongwe* (Nesbitt et al., 2020), and sulcimentisaurians (e.g., *S. opolensis*: Dzik, 2003; *Sacisaurus agudoensis*: Langer & Ferigolo, 2013). The femoral head is anteromedially oriented, forming an angle of approximately 70° with the transverse axis of the distal end. In anterolateral view, the femoral head is sub-rectangular in contour due to the angled greater trochanter. In the center of the anterior surface of the head, distal to the proximal articular surface, there is a large and rugose additional ossification that represents the anterolateral scar (sensu Griffin & Nesbitt, 2016) for the insertion of the iliofemoral ligament (Figure 10). Posterodistally to it, a subvertically oriented dorsolateral trochanter (=obturator ridge) is placed approximately 5 mm distal to the proximal margin of the femur. This ridge is anteroposteriorly thick, tapers distally, and reaches the trochanteric shelf in PULR V-111. By contrast, the dorsolateral trochanter finishes distally before reaching the trochanteric shelf in the smaller PULR V-113. The dorsolateral trochanter may represent either the site of insertion of *M. puboisquiofemoralis externus* (Hutchinson, 2001) or *M. iliotrochantericus* (Langer, 2003).

The anterior trochanter (=lesser trochanter) is a subtriangular, proximally pointed, and mound-like process positioned at the lateral surface of the femur. This trochanter gradually merges proximally with the rest of the bone, lacking a cleft separating it from the shaft, and may constitute the site of insertion of *M. iliotrochantericus caudalis* (Hutchinson, 2001). A shallow depression excavates the surface lateral to the trochanter in PULR V-111 (Figure 10d), but this seems to be absent in PULR V-113, although its absence could be an artifact of the taphonomic anteromedial compression of the bone. From the base of the anterior trochanter, a subtle trochanteric shelf extends laterodistally, curves distally on the posterior surface of the bone, and continues in that direction as a sublongitudinal ridge. This crest is hypothesized to represent the site of insertion of *M. iliofemoralis externus* (Hutchinson, 2001; Langer, 2003). The fourth trochanter is completely covered with matrix in both specimens.

The anterior surface of the distal end of the femur lacks distinct muscle scars. Only the very base of the medial condyle is preserved and the surfaces are rather damaged. In distal view, the anterior margin is strongly convex along its whole extension, lacking an extensor fossa. The medial condyle occupies approximately the medial half of the distal end and it is separated from the lateral condyle by a broad, moderately deep, and distally-opened fossa ("ig" in Figure 9H). By contrast, the anterior half of the distal surface of the bone is distinctly convex. That concavity may represent the site of insertion of the posterior cruciate ligaments (Currie & Zhao, 1993). It extends posterolaterally as a shallow groove that separates the lateral condyle from the tibiofibular crest. This groove is restricted to the distal surface and results in an incipiently concave transition between the lateral condyle and the tibiofibular crest in lateral view. This condition resembles that of *A. kongwe* (Nesbitt et al., 2020) and the holotype of "*Pseudolagosuchus major*" (PVL 4629), but differs from that of some other early dinosauriforms (e.g., *L. talampayensis*: Sereno & Arcucci, 1994; *S. opolensis*: Dzik, 2003), in which both structures are separated by a deep lateral concavity The tibiofibular crest is posteriorly oriented and subtriangular in distal view. The lateral margin of the lateral condyle is continuously convex in distal view.

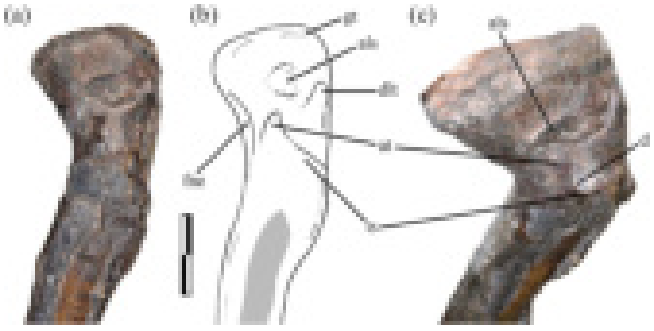

FIGURE 10 Detail of proximal end of left femur of *Lewisuchus admixtus* (PULR V-111) in: (a,b), lateral and (c), proximoanterolateral views. References: at, lesser trochanter; d, depression; dlt, dorsolateral trochanter; fls, anterolateral scar; fne, femoral neck; gt, greater trochanter; ts, trochanteric shelf. Scale bar: 1 cm for a and b; c not to scale

5.29 | Tibia

A complete left tibia is preserved in PULR V-111 (Figure 11; Table 6) and the proximal portion plus a shaft fragment of the right tibia are preserved in PULR V-113 (Table 8). Both bones are somewhat deformed as a result of taphonomic transverse compression. The cnemial crest is straight and anteriorly oriented in proximal view, and shorter anteroposteriorly than the medial condyle. In lateral and medial views, the crest projects slight both anteriorly and proximally. It is separated from the posterior condyles by a very deep, proximolaterally facing fossa. In proximal view, the cnemial crest is separated from the posterior condyles by lateral and medial shallow

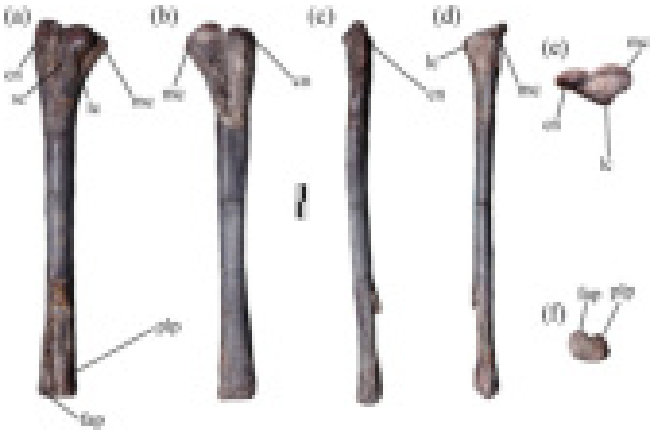

FIGURE 11 Left tibia of *Lewisuchus admixtus* (PULR V-111) in: (a), lateral; (b), medial; (c), anterior; (d), posterior; (e), proximal, and (f), distal views. References: cn, cnemial crest; fap, facet for the ascending process of the astragalus; lc, lateral condyle; mc, medial condyle; plp, posterolateral process; sc, thick and rugose longitudinal muscle scar. Scale bar: 1 cm

concavities. However, the medial concavity, although present in both specimens, seems to result from the collapse of cortical bone. The anterior margin of the cnemial crest is rounded in lateral view. The lateral condyle is anteriorly positioned when compared to the medial one, but still posterior to the anteroposterior center of the proximal end of the bone. The lateral condyle has a rounded lateral margin in proximal view and its proximal surface is anteroposteriorly convex and positioned distal to that of the medial condyle. The latter has an anteroposteriorly convex and transversely concave proximal surface, with a medial edge distinctly raised from the rest of the proximal surface of the bone. The medial condyle has a convex medial margin in proximal view and is anteroposteriorly longer than the lateral condyle. Both posterior condyles are separated posteriorly from one another by an obtuse angle, but there is no groove between them. The lateral surface of the proximal portion of the bone possesses a thick and rugose longitudinal scar that contacts proximally the anterolateral corner of the lateral condyle. The position and extension of this scar matches that of the low longitudinal tuberosity present in several early saurischians (e.g., *S. tupiniquim*: Langer, 2003; *Eoraptor lunensis*: Sereno, Martínez, & Alcober, 2013; *Chromogisaurus novasi*: Ezcurra, 2010) and the flange-like fibular crest of some silesaurids (e.g., *S. opolensis*: Dzik, 2003) and neotheropods (e.g., *Liliensternus liliensterni*: MB R.2175; *Dilophosaurus wetherilli*: Marsh & Rowe, 2020). We interpret these structures as different developments of the same homologous feature. The lateral longitudinal scar is more laterally prominent and slightly broader in PULR V-113. Immediately distal to the longitudinal scar, there is a nutritious foramen for the passage of the cranial tibial artery (Baumel & Witmer, 1993), which extends proximally as a shallow groove. The tibial shaft is oval in cross-section, with an anteroposterior main axis, although the degree of transverse compression of the bone is likely exaggerated by deformation.

The tibia expands slightly and gradually anteroposteriorly and medially toward its distal end. As a result, its distal outline is broader anteroposteriorly than lateromedially, a condition that could be due to the lateromedial compression of the bone because other specimens of *L. admixtus* possess subquadrangular tibiae in distal view (Ezcurra, Nesbitt, Fiorelli, et al., 2020; Novas, 1989). The lateral surface of the distal end of the bone possesses a deep and narrow longitudinal groove that opens distally into a notch. This groove is slightly displaced anteriorly at its proximal end, but it becomes centered anteroposteriorly at the distal margin of the bone, where it separates the anterolateral (the facet for the reception of the ascending process of the astragalus) and the posterolateral (=lateral malleolus) processes. The posterolateral process of the tibia extends laterally up to the same level as the facet for the ascending process of the astragalus and possesses a transversely convex, laterodistally facing articular surface. This process has a lobular profile in posterior view. The facet for reception of the ascending process of the astragalus is also transversely convex, closely resembling the condition of the posterolateral process. The medial portion of the distal articular surface of the bone is slightly concave anteroposteriorly. As a result, the astragalar articulation in the tibia is shallowly concave on its medial third and convex on its lateral two-thirds.

5.30 | Astragalus

The left astragalus of PULR V-111 is nearly complete, with the exception of a missing posterolateral corner (Figure 12; Table 9). The bone is asymmetric in proximal/distal views, with its medial portion more anteriorly expanded than the lateral. The anterior surface of astragalus is concave and its deepest region is laterally displaced from the level of mid-width of the bone. This concavity would have received the proximal surface of distal tarsal 3 and the slight anterior expansion lateral to it would have articulated with part of distal tarsal 4. The anterior surface of the astragalus possesses a dorsally curved groove that is slightly medially and ventrally displaced from the center of this surface. The ventral surface of the bone is anteroposteriorly and slightly transversely convex. The posterior surface is also convex along all its

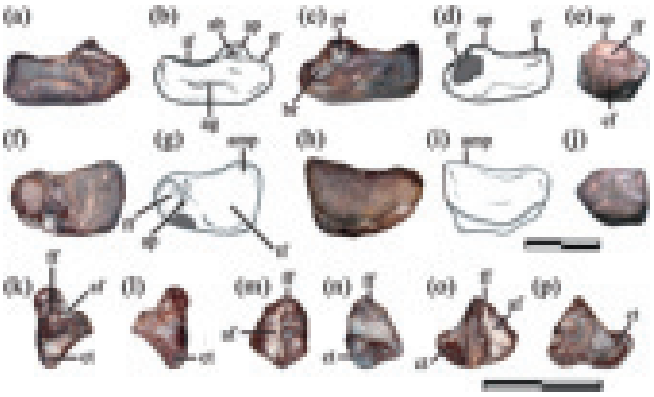

FIGURE 12 Left astragalus (a–j) and calcaneum (k–p) of *Lewisuchus admixtus* (PULR V-111) in: (a,b,m), anterior; (c,d,n), posterior; (f,g,k), dorsal; (h,i,l), ventral; (e,p), lateral; and (j,o), medial. References: af, facet for articulation with astragalus; ah, anterior hollow; ag, anterior groove; amp, anteromedial process; ap, ascending process; br, brakeage; cf, facet for articulation with calcaneum; ct, calcaneal tuber; ff, fibular facet; pi, pit; tf, tibial facet. Scale bars: 1 cm

TABLE 9 Measurements (in mm) of the left astragalus and calcaneum of *Lewisuchus admixtus* (PULR V-111)

	Astragalus	Calcaneum
Width	14.7	6.1
Height	7.7	5.1
Depth	9.5	7.1
Width of tibial facet	8.6	—
Oblique width of fibular facet	3.4	(3.0)

Note: Values between brackets indicate incomplete measurements (due to postmortem damage) and the value given is the maximum measurable. Maximum deviation of the calliper is 0.02 mm but measurements were rounded to the nearest 0.1 mm. Width refers to transverse width and depth to anteroposterior depth.

preserved transverse extension. A very shallow transverse groove that curves slightly posteriorly represents the most lateral extension of the medioventral notch for reception of the medial process of the calcaneum. Immediately anterodorsally to this groove there is a ball-shaped articular facet that articulates with a socket on the medial surface of the calcaneum, representing a crocodile-normal crurotarsal ankle joint, as occurs in pseudosuchians and most nondinosaurian avemetatarsalians (Nesbitt et al., 2017). The medial surface of the astragalus is subvertically oriented, where the anterior portion of the bone is taller than the posterior. This surface is anteroposteriorly and dorsoventrally convex, and possesses a slightly medially inflated crescent-shaped prominence adjacent to the anteromedial corner of the bone.

In dorsal view, the anteromedial margin of the astragalus is acute, which represents a derived condition of Dinosauriformes (Langer & Benton, 2006; Novas, 1996). The fibular facet is sub-circular, well-defined and slightly concave; delimited anteriorly and posteriorly by low and well-defined edges. This surface represents approximately one third of the transverse width of the articular surface for the tibia. The articulation for the tibia is continuous with that for the fibula along the ascending process of the astragalus and posteriorly to it they are separated by a nonarticular surface. This nonarticular surface is represented as a deep fossa, but this condition seems to be the result of damage. The ascending process of the astragalus is developed as an anteroposteriorly oriented crest that becomes shallower posteriorly. This process is distinctly shorter than the astragalar body and it is separated from the anterior surface of the bone by an anterolaterally to posteromedially oriented groove. The depth of this groove is probably exaggerated by damage. The tibial facet is concave along most of its extension, but it becomes slightly anteroposteriorly convex close to the medial margin of the bone. The extension of the tibial facet onto the ascending process of the astragalus results in a more laterally developed facet on the anterior two-thirds of the bone than posteriorly.

5.31 | Calcaneum

The calcaneum is a sub-pyramidal bone distinctly smaller than the astragalus (Figure 12; Table 9). Its medial surface bears the articular facets of the astragalus, which are composed of an anteromedially facing concavity and a posteriorly restricted medial projection. The dorsal surface of the calcaneum possesses a slightly convex articular facet for the fibula that is positioned immediately dorsolateral to the astragalar facet. There is a short, but prominent, calcaneal tuber that projects posteriorly on the posterolateral corner of the bone. There is no depression or groove separating the calcaneal tuber from the rest of the bone on the ventral surface of the calcaneum, neither a depression on the posterior margin of the tuber. The posterior surface of the calcaneum immediately medial to the calcaneal tuber is deeply depressed. The lateral surface is convex and interrupted by a circular, deep, and blind pit on its center. The ventral surface of the calcaneum is flat to slightly convex. The anterior surface of the bone is convex, and articulated with distal tarsal 4.

6 | DISCUSSION

Currently, eight specimens of *L. admixtus* are available, yielding information on skull, mandible, cervical, dorsal, sacral, and caudal vertebrae, ribs, gastralia, pectoral

girdle and forelimbs (except manus), and pelvic girdle and hindlimbs. In other words, this taxon constitutes one of the best-known early dinosauriforms, inviting review of the characteristics uniting it with dinosauriforms other than *L. talampayensis*.

6.1 | Comparisons and implications for the evolution of early dinosauriform character states

The new specimens described here and referred to *L. admixtus* (see Section 4) include bones that are more completely preserved than in the hypodigm of the species (postorbital, sacral vertebrae, ilium, and ischium) or were previously unknown (gastralia; Bittencourt et al., 2014; Ezcurra, Nesbitt, Fiorelli, et al., 2020; Romer, 1972). In addition, the cranial bones of PULR V-111 are well-preserved and add valuable information to an anatomical region poorly known in other early dinosauriforms (Langer et al., 2013). Along this section, we will compare the new specimens of *L. admixtus* with other early dinosauriforms and dinosaurs.

The postorbital is a bone known only in a few non-dinosaurian dinosauriforms (e.g., *A. kongwe*, *S. opolensis*; Dzik & Sulej, 2007; Nesbitt et al., 2020). The postorbital of *L. admixtus* has a flange that slightly projects into the orbit. A very similar flange is also present in several early dinosaurs, such as *E. lunensis* (Sereno et al., 2013), *B. schultzi* (Müller et al., 2018), *Lesothosaurus diagnosticus* (Porro, Witmer, & Barrett, 2015), *Pampadromaeous barberenai* (ULBRA-PVT016), *S. tupiniquim* (MCP 3845-PV), and *Plateosaurus trossingensis* (Prieto-Márquez & Norell, 2011), as well as in the silesaurid *S. agudoensis* (Langer & Ferigolo, 2013). This flange is absent in other early archosauriforms, but the current lack of knowledge about the postorbital morphology in other early avemetatarsalians (e.g., aphanosaurs: Nesbitt et al., 2017; lagerpetids: Ezcurra, Nesbitt, Bronzati, et al., 2020) precludes determining in which node this character state was acquired or how many times it appeared in the evolution of the group.

The lateral surface of the main body of the postorbital of PULR V-111 possesses a sub-horizontal ridge that is confluent with the orbital margin of the bone, closely resembling the condition in the holotype of the species (PULR 01). A similar crest is present in some non-avemetatarsalian archosauriforms (e.g., *Chanaresuchus bonapartei*: PULR 01; *Gracilisuchus stipanicicorum*: MCZ 4117), but it is absent in most early dinosauriforms and dinosaurs (e.g., *S. agudoensis*: Langer & Ferigolo, 2013; *E. lunensis*: Sereno et al., 2013; *L. diagnosticus*: Porro et al., 2015), with the possible exception of *B. schultzi* that has a narrow and shallow ridge on the lateral surface of the posterior process (Müller et al., 2018).

The squamosal of *L. admixtus* resembles in general morphology those of the nondinosaurian dinosauriforms *A. kongwe* (Nesbitt et al., 2020) and *S. opolensis* (ZPAL Ab 1930/92/25), including the acute angle formed between the ventral and anterior processes in lateral view. As a result, the infratemporal fenestra of these species should have had a posterior constriction at mid-height (see Dzik & Sulej, 2007: fig. 20a). The lateral surface of the base of the ventral process is separated from the rest of the bone by a thick ridge in *L. admixtus*, *S. opolensis* (ZPAL Ab 1930/92/25), and some early dinosaurs (e.g., *P. trossingensis*: Prieto-Márquez & Norell, 2011), but such a ridge is absent in *A. kongwe* (Nesbitt et al., 2020). These character states cannot be observed in the squamosal of the holotype of *L. admixtus* because of damage.

One of the most outstanding features of the quadrate of *L. admixtus* is its strong posterior curvature, especially toward its ventral end. The orientation of the quadrate shaft, together with the morphology of the quadratojugal articulation, suggests that the posterior region of the skull was relatively low. This condition can be also observed in the holotype specimen (PULR 01), as noted by Bittencourt et al. (2014). In sum, the information provided by the PULR V-111 lends support to the reconstruction of the skull performed by Romer (1972), Paul (1988), and Ezcurra, Nesbitt, Bronzati, et al. (2020) depicting the skull of *L. admixtus* as very low and elongated.

Bonaparte (1975) recognized a series of character states shared between *L. talampayensis* and saurischian dinosaurs, including the presence of a sharp morphological zonation of the vertebral column. Bonaparte (1975) interpreted this modification in the axial skeleton as probably one of the most important traits to characterize the dinosaur lineages. In fact, such zonation is poorly developed or absent in other archosauriforms, including well-preserved skeletons of species that are contemporaneous of *L. talampayensis*, such as *G. stipanicicorum* and *C. bonapartei*. Subsequent authors (Gauthier, 1986; Novas, 1996; Stefanic & Nesbitt, 2019) corroborated such zonation in the transition between cervical and dorsal vertebrae as one of the most important conditions to characterize Dinosauria and their immediate precursors.

The new specimen of *L. admixtus* PULR V-111 has a marked vertebral zonation, supporting the original proposal of Bonaparte (1975), who recognized three sections in the presacral vertebral column of *L. talampayensis*: cervical, cervico-dorsal, and dorsal. In *L. admixtus*, the vertebral column of PULR V-01 and PULR V-111 allow recognizing five different regions with unique characteristics: (a) cervical vertebrae 5–8, with strongly elongated

and ventrally keeled centra, and elongated and anterodorsally oriented prezygapophyses, (b) cervical vertebra 9, with a short centrum without ventral keel, well-developed laminae, and postzygapophyseal-centrodiapophyseal fossa, (c) dorsal vertebrae 1–2, with short centra without lateral excavations, and neural arch with sharp laminae, (d) dorsal vertebrae 3–4, with tall, anteroposteriorly expanded and anterodorsally oriented neural spines, with thick spine tables, and (e) dorsal vertebrae 5–10, with low and long centra, lacking lateral excavations, and sub-vertically oriented, fan-shaped neural spines that bear transversely narrow spine tables. This vertebral zonation, composed for at least five different morphotypes, has not been previously reported in other early dinosauriforms, including *L. talampayensis*. This may be in part consequence of the exceptional preservation and skilful technical preparation of PULR V-111, which permitted recognizing details such as the differential depth of the vertebral fossae and laminae. It is possible that new specimens and more detailed studies will allow identifying vertebral zonations similar to that of *L. admixtus* in other early dinosauriforms that still remain poorly known.

L. talampayensis and *L. admixtus* share sub-horizontally oriented and elongated prezygapophyses on their dorsal vertebrae that, coupled with the partially overlapping and fan-shaped neural spines, may have stiffened the dorsal column of these animals (Bonaparte, 1975). On the other hand, in other early dinosauriforms, including *S. opolensis*, the neural spines have sub-parallel anterior and posterior margins, resulting in a sub-rectangular contour when viewed laterally (Piechowski & Dzik, 2010). The condition shared by *L. talampayensis* and *L. admixtus* is unique among early dinosauriforms.

Bittencourt et al. (2014) inferred that *L. admixtus* had seven cervical vertebrae, an equivalent count to that interpreted by Piechowski and Dzik (2010) for *S. opolensis*. However, it is worth to mention that the cervico-dorsal transition in the specimen described by the latter authors is damaged, and this vertebral count might be considered tentative. Bonaparte (1975) described a cervical count of nine elements for *L. talampayensis* on the basis of two articulated and well-preserved specimens. In this species, the posterior cervical vertebrae are characterized by having relatively short and tall centra, with anterior and posterior articular surfaces set at different dorsoventral levels, anteriorly oriented neural spines, and dorsally oriented prezygapophyses that extend beyond the level of the anterior margin of the centrum (Bonaparte, 1975). This set of features is present in the elements identified by Bittencourt et al. (2014) as the first dorsal vertebra in the holotype of *L. admixtus*. The element identified by Bittencourt et al. (2014) as the second dorsal vertebra possesses a long rib in articulation, which could be interpreted as indicating the beginning of the thoracic region. Nevertheless, the tuberculum of this rib articulates with a parapophysis positioned on the anteroventral corner of the centrum, which is interpreted here as evidence that it corresponds to a cervical vertebra. Hence, we infer that the holotype of *L. admixtus* has a minimal cervical count of nine vertebrae, which is in agreement with the condition inferred for PULR V-111.

The ilia of the new specimens of *L. admixtus* add valuable information previously unknown for the species. The ilium differs from that of *L. talampayensis* in the presence of a brevis fossa, which has been recovered as a synapomorphy of Dracohors (Silesauridae + Dinosauria) by Nesbitt et al. (2010). The brevis fossa of *L. admixtus* is relatively deep and has a more ventral, rather than a predominantly lateral orientation, resembling the condition of some silesaurids (e.g., *A. kongwe* and *S. opolensis*) and early dinosaurs (e.g., *S. tupiniquim* and *C. novasi*; Nesbitt et al., 2020). On the contrary, in deeply nested silesaurids as *S. agudoensis* and herrerasaurids such as *H. ischigualastensis* and *Gnathovorax cabreirai* the brevis fossa is represented by a poorly defined furrow and is almost laterally oriented (Dzik, 2003; Langer & Ferigolo, 2013; Novas, 1994; Pacheco et al., 2019). This indicates that the evolution of the brevis fossa is not as straightforward as previously thought and that the diversity and variation of this anatomical feature is probably far from being well-known.

As occurs in early dinosaurs, *L. admixtus* possesses elongated ischium and pubis (representing at least 2/3 of the femoral length). Novas (1991) recognized an elongated pubis as synapomorphic of the clade composed of "*Pseudolagosuchus major*" and Dinosauria. However, recent findings indicate that the distribution and synapomorphic condition of this feature is uncertain; a very elongate pubis that extends more than 2/3 of the femoral length is also present in aphanosaurs (Nesbitt et al., 2019), but the bone is shorter in some early-diverging dinosaurs, such as the herrerasaurs *Gnathovorax cabrerai* and *Staurikosaurus pricei* (Pacheco et al., 2019). This indicates that the distribution of this character is complex, at least at base of Pan-Aves. A phylogenetic analysis, that is beyond of the scope of present contribution, will probably shed some light on the status of pubic elongation as a synapomorphy of the clade uniting *L. admixtus* and Dinosauria.

The femur of PULR-V 111 possesses a well-developed dorsolateral trochanter, as also occurs in the silesaurids *S. opolensis*, *A. kongwe*, and *S. agudoensis* (Griffin & Nesbitt, 2016; Langer & Ferigolo, 2013; Nesbitt, 2011)

and several early saurischians, such as *Guaibasaurus candelarensis*, *S. tupiniquim*, and *E. lunensis* (Bonaparte, Ferigolo, & Ribeiro, 1999; Langer, 2003; Sereno et al., 2013). Nesbitt (2011) proposed that the presence of a dorsolateral trochanter was diagnostic of Dracohors (Silesauridae + Dinosauria), and Hutchinson (2001) considered it as the insertion site for a portion of *M. puboischiofemoralis internus* and, as a consequence, as part of the greater trochanter (*contra* Bonaparte et al., 1999).

The morphology of the tibia of the new specimens of *L. admixtus* is congruent with that of the holotype (PULR 01). It is interesting to highlight the presence of a longitudinal, raised scar on the lateral surface of the proximal end of the bone in both specimens. Based on the topological congruency with the tuberosity and crest present in silesaurids and dinosaurs (e.g., *S. opolensis*, *S. tupiniquim*, and *H. ischigualastensis*), we interpret these structures as homologous.

The proximal tarsals of *L. admixtus* are similar to those of *L. talampayensis* and *A. kongwe* in many anatomical details, but differ from deeply nested silesaurids (e.g., *S. opolensis*) and early dinosaurs in the better developed medial process and calcaneal tuber of the eponymous bone. The tibial articular surface in the astragalus is divided into two basins, a concave medial portion and a convex lateral one. This flexed tibial facet resembles the condition present in *L. talampayensis* and early pseudosuchian archosaurs (Nesbitt, 2011).

6.2 | Synonymy between *L. admixtus* and "*Pseudolagosuchus major*"

Arcucci (1987) described the new genus and species "*Pseudolagosuchus major*" on the basis of a hypodigm composed of four very incomplete, but informative, specimens coming from the same stratigraphic levels and locality as the holotype of *L. admixtus* (Arcucci, 1987; Romer, 1972). The holotype of "*Pseudolagosuchus major*" (PVL 4629; Figure 13) is poorly preserved and has few informative characters. However, main anatomical character states are congruent with those of the new specimens of *L. admixtus* described here, and these specimens are, in turn, congruent with the holotype of *L. admixtus*. The tarsal elements are strongly damaged in the holotype of "*Pseudolagosuchus major*," and the recognition of characters is difficult. In one of the previously referred specimens of "*Pseudolagosuchus major*" (MACN-Pv 18954; Arcucci, 1987), the astragalus and calcaneum are well-preserved and very similar in proportions and general morphology to those of PULR V-111. Indeed, both share an astragalus with a dorsally curved groove on the anterior surface (Arcucci, 1987) and an inflated area on the anterior portion of the medial surface. These characters are absent in other early dinosauriforms that we are aware. The presence of osteoderms dorsal to the neural spines in the anterior presacral series and anteroposteriorly expanded dorsal neural spines is a combination of character states shared between PULR V-111 and the holotype of *L. admixtus*. The unique combination of features that PULR V-111 shares with the holotype of *L. admixtus* and MACN-Pv 18954 are not preserved in the specimen (CRILAR-Pv 552) described by Ezcurra, Nesbitt, Fiorelli, et al. (2020), which was used to formally propose the synonymy between *L. admixtus* and "*Pseudolagosuchus major*." Thus, the new specimens here reported adds more information that supports the assignment of some of the previously referred specimens of "*Pseudolagosuchus major*" to *L. admixtus*.

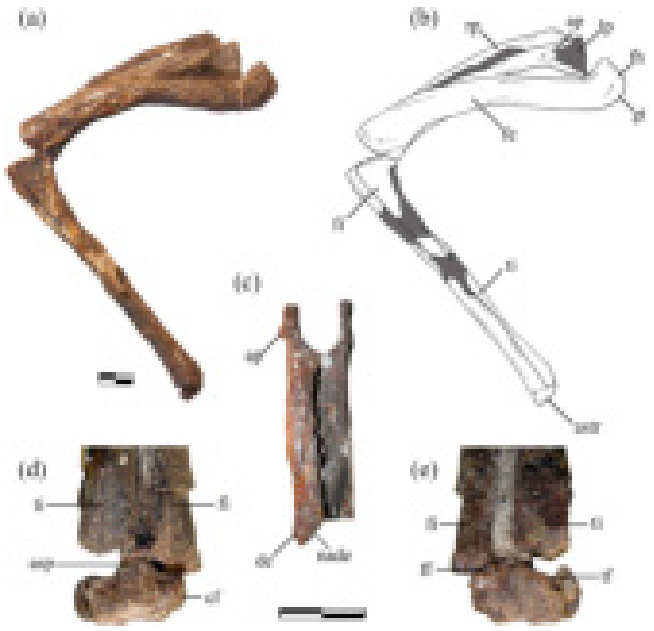

FIGURE 13 Selected bones of the holotype of "*Pseudolagosuchus major*" (PVL 4629). Pubes and left partial hindlimb in (a,b), left lateral view; (c), both pubes in anterior view; and left distal end of tibia and fibula and astragalus in (d), anterior and (e), posterior views. References: ap, ambiens process; asp, ascending process; astr, astragalus; de, distal end; fe, left femur; fh, femoral head; fi, left fibula; gt, greater trochanter; lp, left pubis; rp, right pubis; ti, left tibia. Scale bars: 1 cm

7 | CONCLUSIONS

New specimens reported here add valuable information on the anatomy of *L. admixtus*. Outstanding novel features described here for this taxon include an iliac portion of the acetabulum that is medially closed, elongated

ischium and pubis (representing at least 2/3 of the femoral length), fan-shaped dorsal neural spines with a spine tables, and gastralia well separated from one another. Besides, the cranial bones, presacral series, femur, tibia, and proximal tarsals of the new specimens match the preserved overlapping anatomy of the holotype of *L. admixtus* and some of the specimens previously referred to "*Pseudolagosuchus major*" (e.g., MACN-Pv 18954), including the presence of unique combination of character states among dinosauriforms. This provides stronger evidence for the association of specimens that currently form the hypodigm of *L. admixtus*. An improved understanding of the anatomy and taxonomy of the Chañares Formation dinosauriforms is crucial to shed new lights on the phylogenetic relationships among nondinosaurian dinosauriforms and the dawn of dinosaur evolution.

ACKNOWLEDGMENTS

The authors thank the late Jaime Powell, Rodrigo González, Carolina Madozzo Jaén, and Pablo Ortiz (Instituto Miguel Lillo) for their assistance during research visits to the PVL collection, and Emilio Vaccari and Gabriela Cisterna (Universidad de La Rioja) for their help during the revision of the PULR collection. The authors also thank J. García Marsá, G. Lio, M. Motta, M. Aranciaga Rolando, S. Rozadilla, J. D'Angelo, and N. Chimento (Museo Argentino de Ciencias Naturales) for comments and discussion about the phylogenetic relationships of early dinosauriforms. The authors are especially indebted to J. F. Bonaparte for fruitful discussions and sharing unpublished data. Special thanks to technicians C. Alsina and F. De Cianni for the skillful preparation of the specimens here studied. This research was partially supported by the Agencia Nacional de Investigaciones Científicas y Técnicas (PICT 2018-1186 to Martín D. Ezcurra; PICT 2018-1390 to Federico Agnolín) and donation from Mr. Coleman Burke (New York) to Fernando Novas. Special thanks to R. Temp Müller and A. Marsh for their comments on the MS.

ORCID

Federico Agnolín https://orcid.org/0000-0001-5073-561X
Federico Brissón Egli https://orcid.org/0000-0001-8037-5467
Martín D. Ezcurra https://orcid.org/0000-0002-6000-6450

REFERENCES

Agnolín, F. L., & Ezcurra, M. D. (2019). The validity of *Lagosuchus talampayensis* Romer, 1971 (Archosauria, Dinosauriformes), from the Late Triassic of Argentina. *Breviora*, *565*(1), 1–21.

Arcucci, A. B. (1987). Un nuevo Lagosuchidae (Thecodontia–Pseudosuchia) de la fauna de Los Chanares (edad reptil Chanarense, Triásico Medio), La Rioja, Argentina. *Ameghiniana*, *24*(1–2), 89–94.

Arcucci, A. B. (1997). Dinosauromorpha. In P. Currie & K. Padian (Eds.), *Encyclopedia of dinosaurs* (pp. 179–184). San Diego: Academic Press.

Arcucci, A. B. (1998). New information about dinosaur precursors from the Triassic Los Chañares Fauna, La Rioja, Argentina. *Journal of African Earth Sciences*, *27*, 9–10.

Arcucci, A. B. (2005). Una reevalución de los dinosauriomorfos basales y el origen de Dinosauria. In *Boletim de Resumos do II Congresso Latino–americano de Paleontologia de Vertebrados* (p. 33). Río de Janeiro: Museu Nacional, Rio de Janeiro, Serie Livros 12.

Baumel, J. J., & Witmer, L. M. (1993). Osteologia. In J. J. Baumel, S. A. King, J. E. Breazile, H. E. Evans, & J. C. Venden Berge (Eds.), *Handbook of avian anatomy: Nomina Anatomica Avium* (2nd ed., pp. 45–132). Cambridge, MA: Publications of the Nuttal Ornithological Club.

Benton, M. J. (1985). Classification and phylogeny of the diapsid reptiles. *Zoological Journal of the Linnean Society*, *84*(2), 97–164.

Bittencourt, J. S., Arcucci, A. B., Marsicano, C. A., & Langer, M. C. (2014). Osteology of the Middle Triassic archosaur *Lewisuchus admixtus* Romer (Chañares Formation, Argentina), its inclusivity, and relationships amongst early dinosauromorphs. *Journal of Systematic Palaeontology*, *13*, 189–219.

Bonaparte, J. F. (1975). Nuevos materiales de *Lagosuchus talampayensis* Romer (Thecodontia–Pseudosuchia) y su significado en el origen de los Saurischia. Chañarense inferior, Triasico Medio de Argentina. *Acta Geologica Lilloana*, *13*, 5–90.

Bonaparte, J. F. (1982). Classification of the Thecodontia. *Geobios*, *15*, 99–112.

Bonaparte, J. F. (1997). *El Triásico de San Juan–La Rioja, Argentina, y sus Dinosaurios*. Buenos Aires: Museo Argentino de Ciencias Naturales 190 p.

Bonaparte, J. F. (1999). Evolución de las vértebras presacras en Sauropodomorpha. *Ameghiniana*, *36*(2), 115–187.

Bonaparte, J. F., Ferigolo, J., & Ribeiro, A. M. (1999). A new Early Late Triassic saurischian dinosaur from Rio Grande do Sul State, Brazil. *National Science Museum Monographs*, *15*, 89–109.

Cabreira, S. F., Kellner, A. W. A., Dias da Silva, S., da Silva, L. R., Bronzati, M., de Almeida Marsola, J. C., … Langer, M. C. (2016). A unique Late Triassic dinosauromorph assemblage reveals dinosaur ancestral anatomy and diet. *Current Biology*, *26*(22), 3090–3095.

Carrano, M. T., & Hutchinson, J. R. (2002). Pelvic and hindlimb musculature of *Tyrannosaurus rex* (Dinosauria: Theropoda). *Journal of Morphology*, *252*, 207–228.

Colbert, E. H. (1970). A Saurischian dinosaur from the Triassic of Brazil. *American Museum Novitates*, *2405*, 1–39.

Cope, E. D. (1869). Synopsis of the extinct Batrachia and Reptilia of North America. *Transactions of the American Philosophical Society*, *14*, 1–252.

Currie, P. J., & Zhao, X. (1993). A new carnosaur (Dinosauria, Theropoda) from the Jurassic of Xinjiang, People's Republic of China. *Canadian Journal of Earth Sciences*, *30*, 2037–2081.

Desojo, J. B., Ezcurra, M. D., & Schultz, C. L. (2011). An unusual new archosauriform from the Middle–Late Triassic of southern Brazil and the monophyly of Doswelliidae. *Zoological Journal of the Linnean Society*, *161*(4), 839–871.

Dzik, J. (2003). A beaked herbivorous archosaur with dinosaur affinities from the early late Triassic of Poland. *Journal of Vertebrate Paleontology*, *23*, 556–574.

Dzik, J., & Sulej, T. (2007). A review of the early Late Triassic Krasiejów biota from Silesia, Poland. *Phytopatologia Polonica*, *64*, 3–27.

Ezcurra, M. D. (2006). A review of the systematic position of the dinosauriform archosaur *Eucoelophysis baldwini* Sullivan & Lucas, 1999 from the Upper Triassic of New Mexico, USA. *Geodiversitas*, *28*(4), 649–684.

Ezcurra, M. D. (2010). A new early dinosaur (Saurischia: Sauropodomorpha) from the late Triassic of Argentina: A reassessment of dinosaur origin and phylogeny. *Journal of Systematic Palaeontology*, *8*, 371–425.

Ezcurra, M. D., Fiorelli, L. E., Martinelli, A. G., Rocher, S., von Baczko, M. B., Ezpeleta, M., ... Desojo, J. B. (2017). Deep faunistic turnovers preceded the rise of dinosaurs in southwestern Pangaea. *Nature Ecology & Evolution*, *1*(10), 1477–1483.

Ezcurra, M. D., Fiorelli, L. E., Trotteyn, M. J., Martinelli, A. G., & Desojo, J. B. (2020). The rhynchosaur record, including a new stenaulorhynchine taxon, from the Chañares Formation (late Ladinian–? Earliest Carnian) of La Rioja Province, northwestern Argentina. *Journal of Systematic Palaeontology*, *18*(23), 1907–1938.

Ezcurra, M. D. & Martínez, R. (2016). Dinosaur precursors and early dinosaurs of Argentina. *Contribuciones del MACN*, Vol. 6, pp. 97–107.

Ezcurra, M. D., Nesbitt, S. J., Bronzati, M., Dalla Vecchia, F. M., Agnolín, F. L., Benson, R. B., ... Langer, M. C. (2020). Enigmatic dinosaur precursors bridge the gap to the origin of Pterosauria. *Nature*, *588*, 445–449.

Ezcurra, M. D., Nesbitt, S. J., Fiorelli, L. E., & Desojo, J. B. (2020). New specimen sheds light on the anatomy and taxonomy of the early Late Triassic Dinosauriforms from the Chañares Formation, NW Argentina. *The Anatomical Record*, *303*, 1393–1438.

Ferigolo, J., & Langer, M. C. (2007). A late Triassic dinosauriform from south Brazil and the origin of the ornithischian predentary bone. *Historical Biology*, *19*(1), 23–33.

Fiorelli, L. E., Ezcurra, M. D., Hechenleitner, E. M., Argañaraz, E., Taborda, J. R., Trotteyn, M. J., ... Desojo, J. B. (2013). The oldest known communal latrines provide evidence of gregarism in Triassic megaherbivores. *Scientific Reports*, *3*(1), 1–7.

Garcia, M. S., Pretto, F. A., Dias-Da-Silva, S., & Müller, R. T. (2019). A dinosaur ilium from the late Triassic of Brazil with comments on key-character supporting Saturnaliinae. *Anais da Academia Brasileira de Ciências*, *91*, e20180614.

García-Marsà, J. A., Agnolín, F. L., & Novas, F. E. (2019). Bone microstructure of *Lewisuchus admixtus* Romer, 1972 (Archosauria, Dinosauriformes). *Historical Biology*, *31*(2), 157–162.

Gauthier, J. A. (1986). Saurischian monophyly and the origin of birds. *Memoirs of the California Academy of Sciences*, *8*, 1–55.

Gauthier, J.A. & de Queiroz, K. (2001). Feathered dinosaurs, flying dinosaurs, crown dinosaurs and the names "Aves". In J. A. Gauthier & L. F. Gall (Eds.) *New perspectives on the origin and early evolution of birds*. Proceedings of the international symposium in honor of John H. Ostrom. New Haven: Peabody Museum of Natural History, Yale University.

Gauthier, J. A., & Padian, K. (2020). Archosauria E.D. Cope [J.A. Gauthier and K. Padian] converted clade name. In K. de Queiroz, P. D. Cantino, & J. A. Gauthier (Eds.), *Pylonyms: A companion of the Phylocode* (p. 1352). Boca Ratón, FL: CRC Press.

Griffin, C. T., & Nesbitt, S. J. (2016). The histology and femoral ontogeny of the Middle Triassic (?late Anisian) dinosauriform *Asilisaurus kongwe* and implications for the growth of early dinosaurs. *Journal of Vertebrate Paleontology*, *36*, e1111224. https://doi.org/10.1080/02724634.2016.1111224

Griffin, C. T., Stocker, M. R., Colleary, C., Stefanic, C. M., Lessner, E. J., Riegler, M., ... Nesbitt, S. J. (2020). Assessing ontogenetic maturity in extinct saurian reptiles. *Biological Reviews*, *96*, 470–525.

Hutchinson, J. R. (2001). The evolution of the pelvic osteology and soft tissues on the line to extant birds (Neornithes). *Zoological Journal of the Linnean Society*, *131*, 123–168.

Klembara, J., & Welman, J. (2009). The anatomy of the palatoquadrate in the lower Triassic *Proterosuchus fergusi* (Reptilia, Archosauromorpha) and its morphological transformation within the archosauriform clade. *Acta Zoologica*, *90*(3), 275–284.

Kokogian, D. S., Spalletti, L. A., Morel, E. M., Artabe, A. E., Martínez, R. N., Alcober, O. A., ... Zavattieri, A. M. (2001). Estratigrafía del Triásico argentino. In A. E. Artabe, E. M. Morely, & A. B. Zamuner (Eds.), *El Sistema Triásico en la Argentina* (pp. 23–54). La Plata: Fundación Museo de La Plata "Francisco Pascasio Moreno".

Langer, M. C. (2003). The pelvic and hind–limb anatomy of the stem–sauropodomorph *Saturnalia tupiniquim* (Late Triassic, Brazil). *PaleoBios*, *23*, 1–40.

Langer, M. C., & Benton, M. J. (2006). Early dinosaurs: A phylogenetic study. *Journal of Systematic Palaeontology*, *4*, 309–358.

Langer, M. C., Ezcurra, M. D., Bittencourt, J. S., & Novas, F. E. (2010). The origin and early evolution of dinosaurs. *Biological Reviews*, *85*, 55–110.

Langer, M. C., & Ferigolo, C. D. (2013). The late Triassic dinosauromorph *Sacisaurus agudoensis* (Caturrita Formation; Rio Grande do Sul, Brazil): Anatomy and affinities. *Geological Society of London, Special Publications*, *379*(1), 353–392.

Langer, M. C., Nesbitt, S. J., Bittencourt, J. S., & Irmis, R. B. (2013). Non-dinosaurian dinosauromorpha. *Geological Society*, *379*(1), 157–186. London: Special Publications.

Mancuso, A. C., & Caselli, A. T. (2012). Paleolimnology evolution in rift basins: The Ischigualasto–Villa Unión Basin (Central–Western Argentina) during the Triassic. *Sedimentary Geology*, *276*, 38–54.

Mancuso, A. C., Gaetano, L., Leardi, J. M., Abdala, F., & Arcucci, A. B. (2014). The Chañares Formation: A window to a middle Triassic tetrapod community. *Lethaia*, *47*, 244–265.

Marsh, A. D., & Rowe, T. B. (2020). A comprehensive anatomical and phylogenetic evaluation of *Dilophosaurus wetherilli* (Dinosauria, Theropoda) with descriptions of new specimens from the Kayenta Formation of northern Arizona. *Journal of Paleontology*, *94*(S78), 1–103.

Marsicano, C. A., Irmis, R. B., Mancuso, A. C., Mundil, R., & Chemale, F. (2016). The precise temporal calibration of dinosaur origins. *Proceedings of the National Academy of Sciences*, *113*(3), 509–513.

Mattar, L. C. B. (1987). Descrição osteólogica do crânio e segunda vértebrata cervical de *Barberenasuchus brasiliensis* Mattar, 1987 (Reptilia, Thecodontia) do Mesotriássico do Rio Grande do Sul, Brasil. *Anais Academia Brasileira de Ciências*, *61*, 319–333.

Milana, J. P., & Alcober, O. A. (1995). Modelo tectosedimentario de la cuenca triásica de Ischigualasto (San Juan, Argentina). *Revista de la Asociación Geológica Argentina*, *49*(3–4), 217–235.

Müller, R. T., Langer, M. C., Bronzati, M., Pacheco, C. P., Cabreira, S. F., & Da Silva, D. S. (2018). Early evolution of sauropodomorphs: Anatomy ad phylogenetic relationships of a remarkably well–preserved dinosaur from the Upper Triassic of southern Brazil. *Zoological Journal of the Linnean Society*, *184*, 1187–1248.

Nesbitt, S. J. (2011). The early evolution of archosaurs: Relationships and the origin of major clades. *Bulletin of the American Museum of Natural History*, *352*, 1–292.

Nesbitt, S. J., Butler, R. J., Ezcurra, M. D., Barrett, P. M., Stocker, M. R., Angielczyk, K. D., … Charig, A. J. (2017). The earliest bird–line archosaurs and the assembly of the dinosaur body plan. *Nature*, *544*, 484–487.

Nesbitt, S. J., Langer, M. C., & Ezcurra, M. D. (2020). The anatomy of *Asilisaurus kongwe*, a dinosauriform from the Lifua Member of the Manda Beds (~ middle Triassic) of Africa. *The Anatomical Record*, *303*(4), 13–873.

Nesbitt, S. J., Langer, M., & Ezcurra, M. D. (2019). The anatomy of asilisaurus kongwe, a dinosauriform from the lifua member of the manda beds (~middle triassic) of africa. *The Anatomicalo Record*, *303*, 813–873.

Nesbitt, S. J., Sidor, C. A., Irmis, R. B., Angielczyk, K. D., Smith, R. M. H., & Tsuji, L. A. (2010). Ecologically distinct dinosaurian sister–group shows early diversification of Ornithodira. *Nature*, *464*, 95–98.

Novas, F. E. (1989). The tibia and tarsus in Herrerasauridae (Dinosauria, incertae sedis) and the origin and evolution of the dinosaurian tarsus. *Journal of Paleontology*, *63*(5), 677–690.

Novas, F. E. (1992). Phylogenetic relationships of the basal dinosaurs, the Herrerasauridae. *Palaeontology*, *35*(1), 51–62.

Novas, F. E. (1994). New information on the systematics and postcranial skeleton of *Herrerasaurus ischigualastensis* (Theropoda: Herrerasauridae) from the Ischigualasto Formation (Upper Triassic) of Argentina. *Journal of Vertebrate Paleontology*, *13*(4), 400–423.

Novas, F. E. (1996). Dinosaur monophyly. *Journal of Vertebrate Paleontology*, *16*, 723–741.

Novas, F.E., Agnolín, F.L. & Ezcurra, M.D. (2015). *Taxonomy of basal dinosauriforms: Evidence provided by a new specimen from the Triassic Chañares Formation*. NW Argentina: V Congreso Latinoamerico de Paleontología de Vertebrados, pp. 58.

Novas, F. E., Agnolín, F. L., Ezcurra, M. D., Müller, R. T., Martinelli, A., & Langer, M. (2021). Review of the fossil record of early dinosaurs from South America, and its phylogenetic implications. *Journal of South American Earth Sciences*, 103341.

Pacheco, C., Müller, R. T., Langer, M., Pretto, F. A., Kerber, L., & da Silva, S. D. (2019). *Gnathovorax cabreirai*: A new early dinosaur and the origin and initial radiation of predatory dinosaurs. *PeerJ*, *7*, e7963.

Paul, G. S. (1988). *Predatory dinosaurs of the world* (pp. 1–464). New York, NY: Simon & Schuster.

Piechowski, R., & Dzik, J. (2010). The axial skeleton of *Silesaurus opolensis*. *Journal of Vertebrate Paleontology*, *30*, 1127–1141.

Porro, L. B., Witmer, L. M., & Barrett, P. M. (2015). Digital preparation and osteology of the skull of *Lesothosaurus diagnosticus* (Ornithischia: Dinosauria). *PeerJ*, *3*, e1494.

Prieto-Márquez, A., & Norell, M. A. (2011). Redescription of a nearly complete skull of *Plateosaurus* (Dinosauria: Sauropodomorpha) from the late Triassic of Trossingen (Germany). *American Museum Novitates*, *3727*, 1–58.

Rogers, R. R., Arcucci, A. B., Abdala, F., Sereno, P. C., Forster, C. A., & May, C. L. (2001). Paleoenvironment and taphonomy of the Chañares formation tetrapod assemblage (Middle Triassic), northwestern Argentina: Spectacular preservation in volcanogenic concretions. *Palaios*, *16*, 461–481.

Romer, A. S. (1971). The Chãnares (Argentina) Triassic Reptile Fauna. XI. Two new long–snouted Thecodonts, *Chanaresuchus* and *Gualosuchus*. *Breviora*, *379*, 1–22.

Romer, A. S. (1972). The Chañares (Argentina) Triassic reptile fauna. XIV. *Lewisuchus admixtus*, gen. et sp. nov., a further thecodont from the Chañares beds. *Breviora*, *390*, 1–13.

Romer, A. S., & Jensen, J. A. (1966). The Chañares (Argentina) Triassic reptile fauna, II. Sketch of the geology Río Chañares – Río Gualo Region. *Breviora*, *252*, 1–20.

Rowe, T. B. (1989). A new species of the theropod dinosaur *Syntarsus* from the early Jurassic Kayenta Formation of Arizona. *Journal of Vertebrate Paleontology*, *9*(2), 125–136.

Sampson, S. D., & Witmer, L. M. (2007). Craniofacial anatomy of *Majungasaurus crenatissimus* (Theropoda: Abelisauridae) from the late cretaceous of Madagascar. *Society of Vertebrate Paleontology, Memoir*, *8*, 32–102.

Sereno, P. C., & Arcucci, A. B. (1993). Dinosaurian precursors from the middle Triassic of Argentina: *Lagerpeton chanarensis*. *Journal of Vertebrate Paleontology*, *13*, 385–399.

Sereno, P. C., & Arcucci, A. B. (1994). Dinosaurian precursors from the Middle Triassic of Argentina: *Lagosuchus talampayensis*, gen. nov. *Journal of Vertebrate Paleontology*, *14*, 53–73.

Sereno, P. C., Martínez, R. N., & Alcober, O. A. (2013). Osteology of *Eoraptor lunensis* (Dinosauria, Sauropodomorpha). *Journal of Vertebrate Paleontology*, *32*, 83–179.

Stefanic, C. M., & Nesbitt, S. J. (2019). The evolution and role of the hyposphene-hypantrum articulation in Archosauria: Phylogeny, size and/or mechanics? *Royal Society Open Science*, *6*(10), 190258.

Stipanicic, P., & Bonaparte, J. F. (1972). Cuenca triásica de Ischigualasto–Villa Unión (Provincias de San Juan y La Rioja). In A. F. Leanza (Ed.), *Geología Regional Argentina* (pp. 507–536). Argentina: Academia Nacional de Ciencias Córdoba.

Tsai, H. P., & Holliday, C. M. (2015). Articular soft tissue anatomy of the archosaur hip joint: Structural homology and functional implications. *Journal of Morphology*, *276*(6), 601–630.

Wilson, J. A. (1999). A nomenclature for vertebral laminae in sauropods and other saurischian dinosaurs. *Journal of Vertebrate Paleontology*, *19*, 639–653.

Wilson, J. A., Michael, D. D., Ikejiri, T., Moacdieh, E. M., & Whitlock, J. A. (2011). A nomenclature for vertebral fossae in sauropods and other saurischian dinosaurs. *PLoS One*, *6*(2), e17114.

Yates, A. M., Wedel, M. J., & Bonnan, M. F. (2012). The early evolution of postcranial skeletal pneumaticity in sauropodomorph dinosaurs. *Acta Palaeontologica Polonica*, *57*(1), 85–100.

How to cite this article: Agnolín, F., Brissón Egli, F., Ezcurra, M. D., Langer, M. C., & Novas, F. (2021). New specimens provide insights into the anatomy of the dinosauriform *Lewisuchus admixtus* Romer, 1972 from the upper Triassic levels of the Chañares Formation, NW Argentina. *The Anatomical Record*, 1–28. https://doi.org/10.1002/ar.24731